some thoughts about...

Extragalactic Astronomy with a deep NIR Large Area Survey

Vladimir Avila-Reese
Instituto de Astronomía, UNAM

The context

(only galaxies/ see other talks for QSO's, clusters, lensing)

There are several competitive current and future 'static' NIR surveys with science drivers focused on EG astronomy *(UKIDSS www.ukidss.org/index.html ,VISTA www.vista.ac.uk/index.html VIRMOS VDS www.oamp.fr/virmos/virmos_vvds.htm, etc.)*

- NIR traces M_s, the galaxy stellar structure, hot dust, and in combination with opt. bands, provide key information about the stellar pop's.
- High-z pop's: e.g., already-in-place at z~1-3 L_* E's are revealed in NIR surveys; SF-ing giant galaxies at z>4-5; growth of structure and bias from z=3 to z=0 // ***but z is crucial!***

What might be the SASSIR strengths?

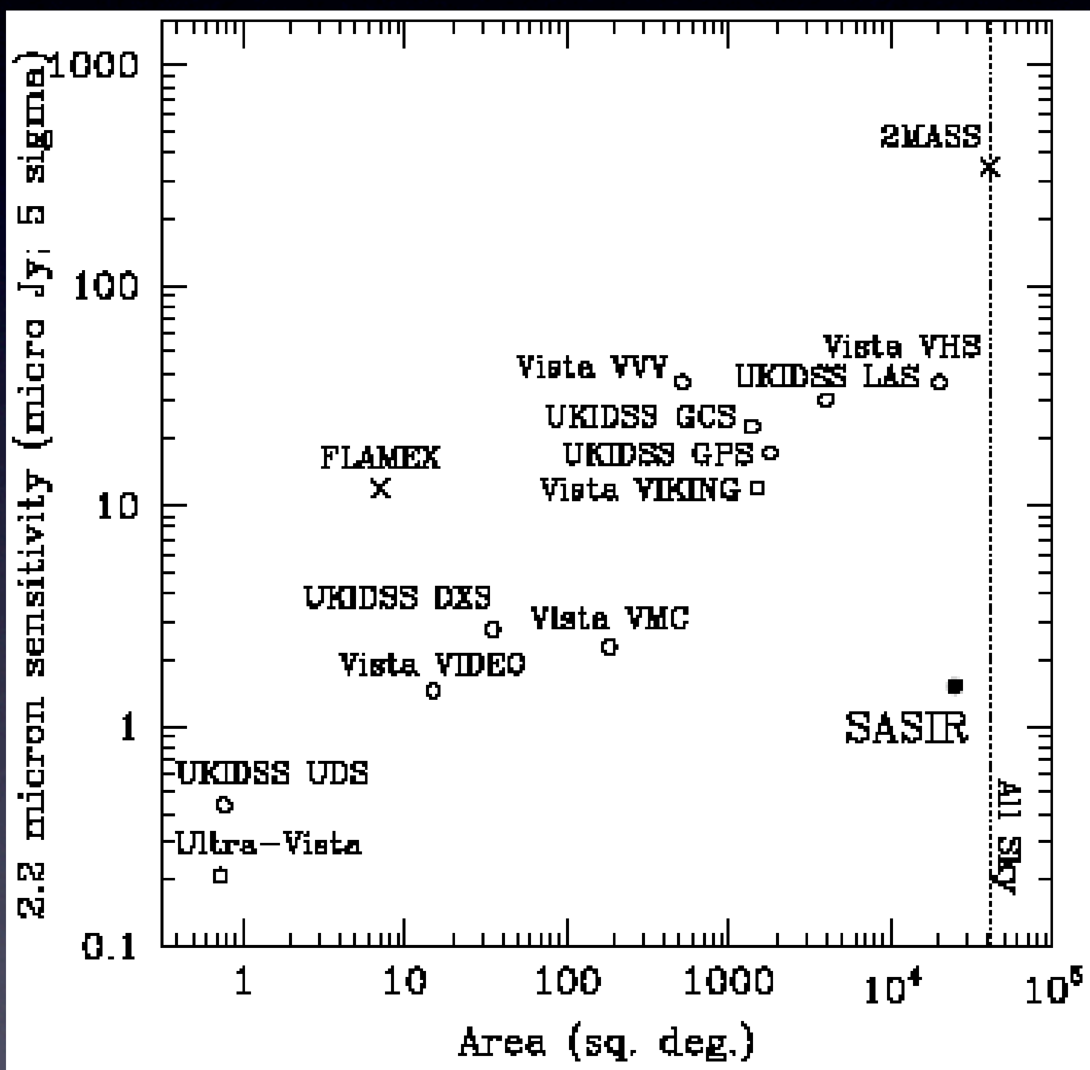

Sensitivity

z~0	z>0
-Low L, low SB pop's *(dIrr, BCD, dSph, LSB).* -Outer galaxy regions (structure, dust)	-Sample completeness down to low L's & SB's (*SMF up to z~4*) -Galaxy evolution *(K~22 for a L_* E at z=3)*

Sky area *(large statistics)*

z~0	z>0
-Morphology (*T, bars, rings, shells,...*) & global structure of gal's (*SB profiles, radii, B/D ratio, CAS, lopsidness*) -Stellar scaling relations -Environment corrtn's	-Clustering of different pop's at different z's -Statistics of rare objects -LSS studies: correlations functions, BAO's, voids & superclusters (ISW)

Spectral range

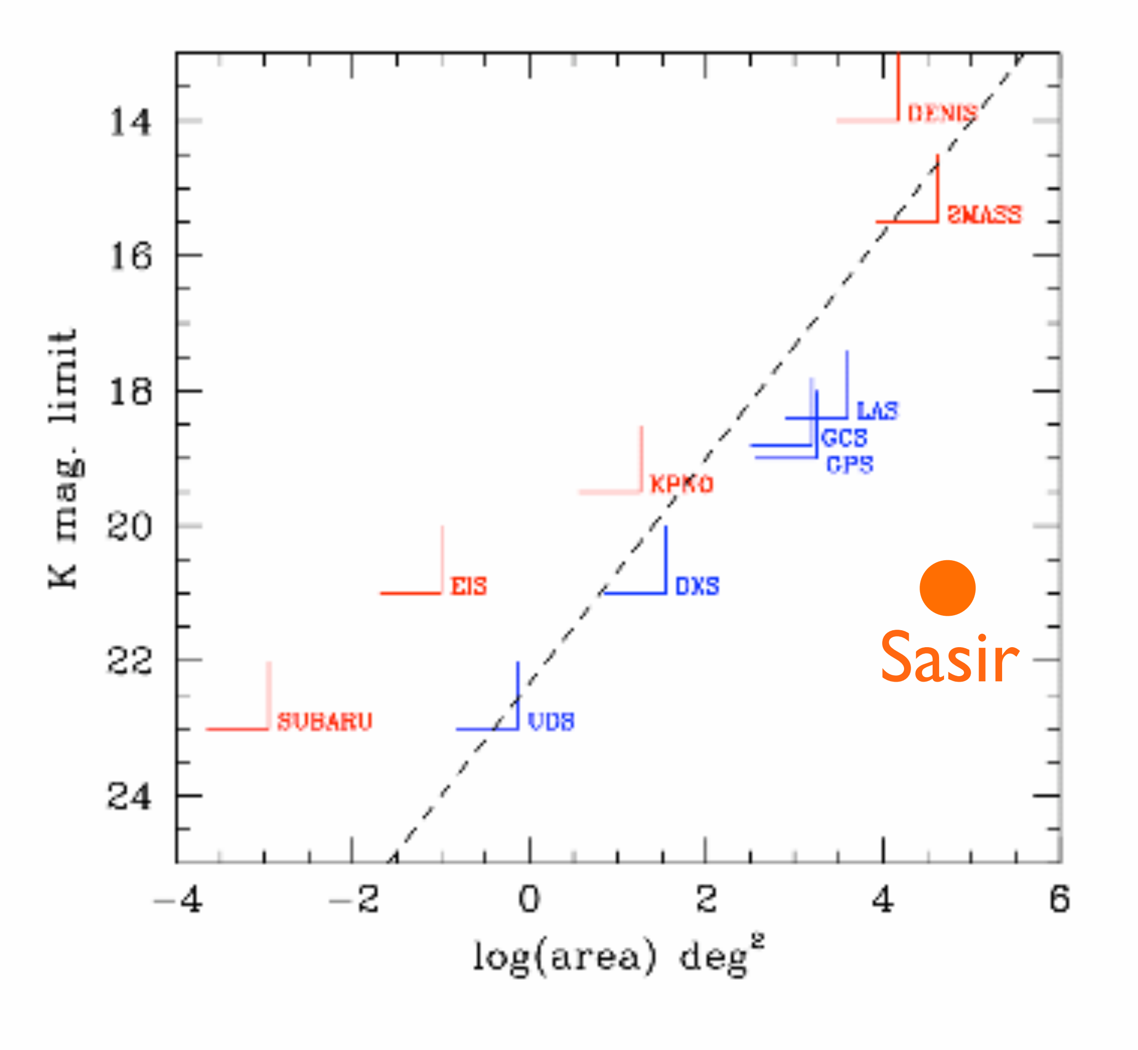

The dashed line shows the Euclidian number counts relation, which goes as $10^{-0.6K}$, i.e. the position of a survey relative to the line is a relative measure of the volume of space surveyed. This illustrates, for example, that for surveys for brown dwarfs 2MASS will detect many more than the KPNO survey, and the LAS is an order of magnitude bigger than 2MASS.

z~0	z>0
-*YJHK color-color* traces SF activity & hot dust -By combining with *opt. bands*, full SP description, *age-Z* degeneracy broken	-NIR color-color diagram may select high-z galaxy pop's (gal. evol.). -*Opt. bands important for photometric z's.*

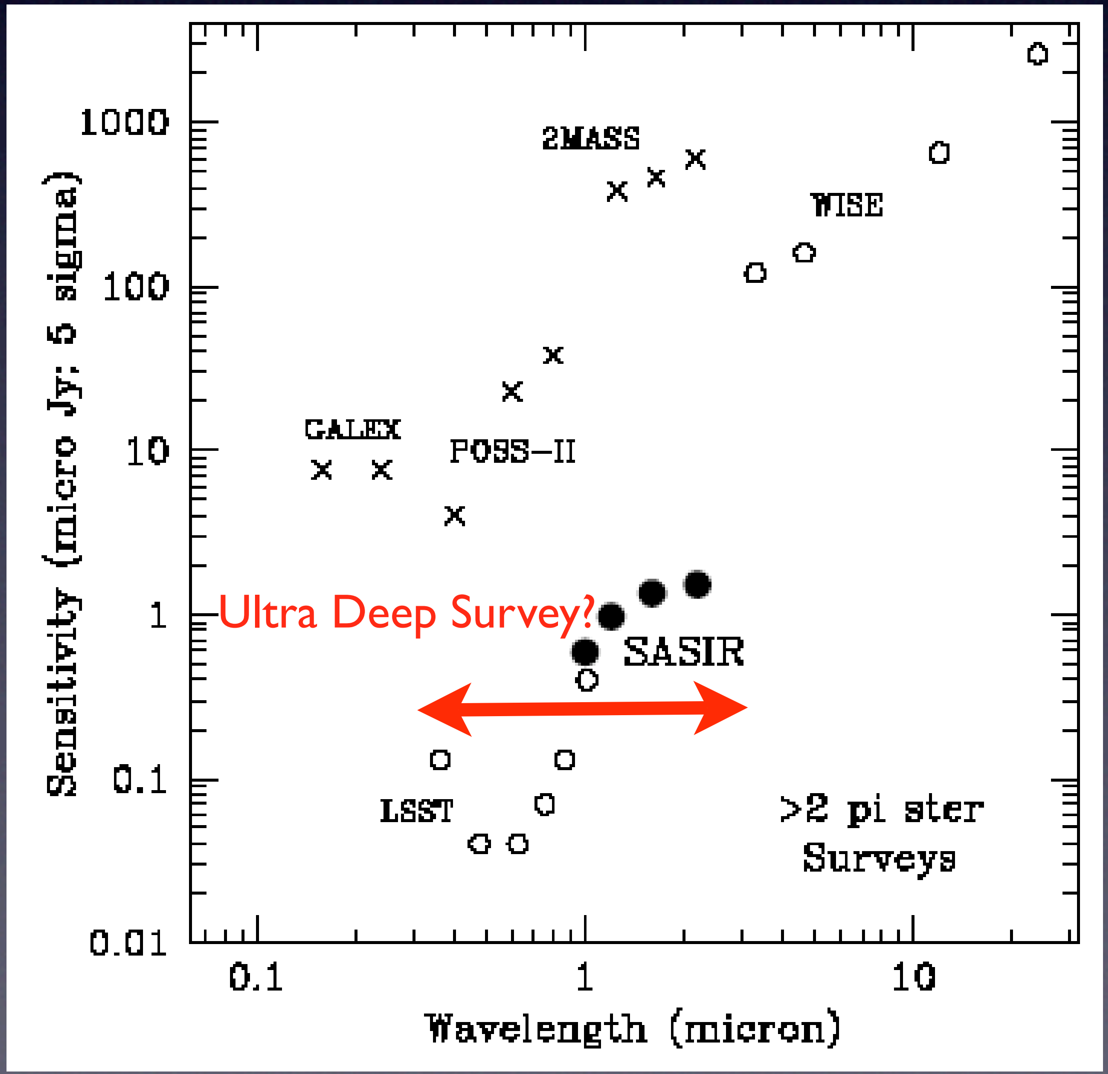

The local universe

☑NIR M/L ~ insensitive to galaxy or stellar type

☑NIR light ~ insensitive to dust extinction

☑K-correction in K-band ~ insensitive to galaxy type ⇒

NIR traces well galaxy Ms & stellar structure

BUT, NIR sky SB (K:14-15) >> outer SB of gal's or even central SB's of low-L and LSB gal's

NIR bands are ideal for inferring stellar (*and eventually baryonic*) galaxy properties and correlations, (i) to be compared with models, and (ii) to determine the 'efficiency' of galaxy and star formation

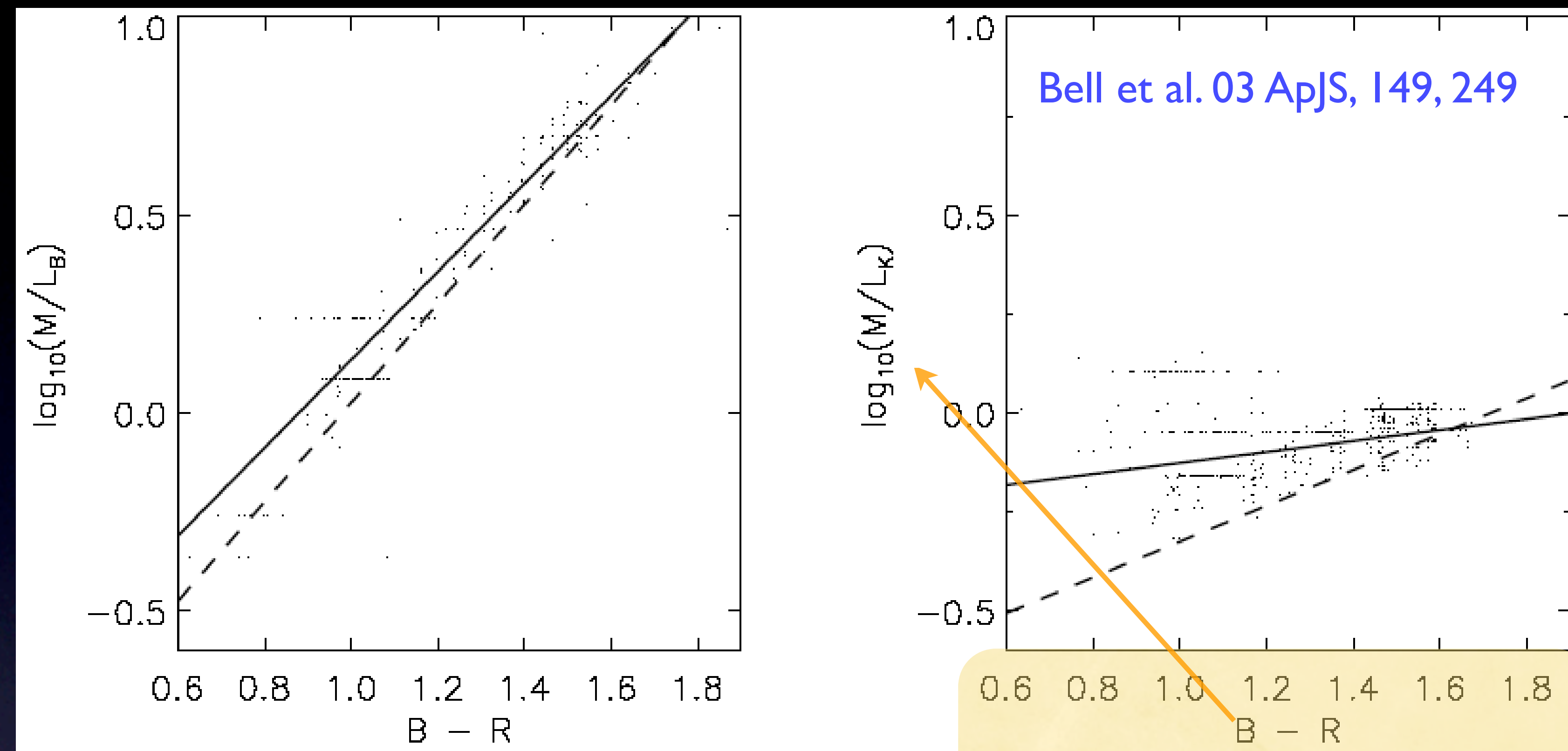

but even in K-band, to estimate Ms, a color is needed!

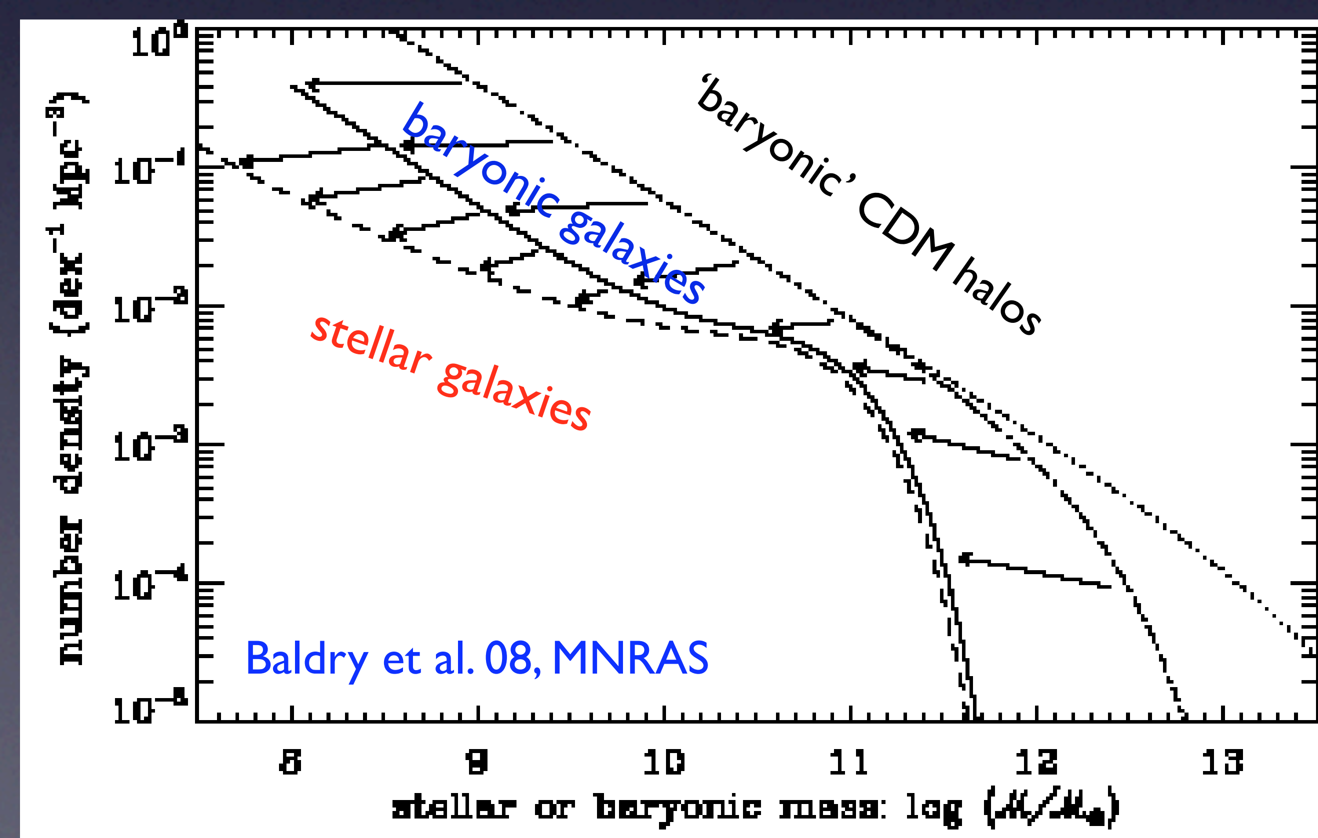

The local universe

☑NIR M/L ~ insensitive to galaxy or stellar type

☑NIR light ~ insensitive to dust extinction

☑K-correction in K-band ~ insensitive to galaxy type ⇒

NIR traces well galaxy Ms & stellar structure

BUT, NIR sky SB (K:14-15) >> outer SB of gal's or even central SB's of low-L and LSB gal's

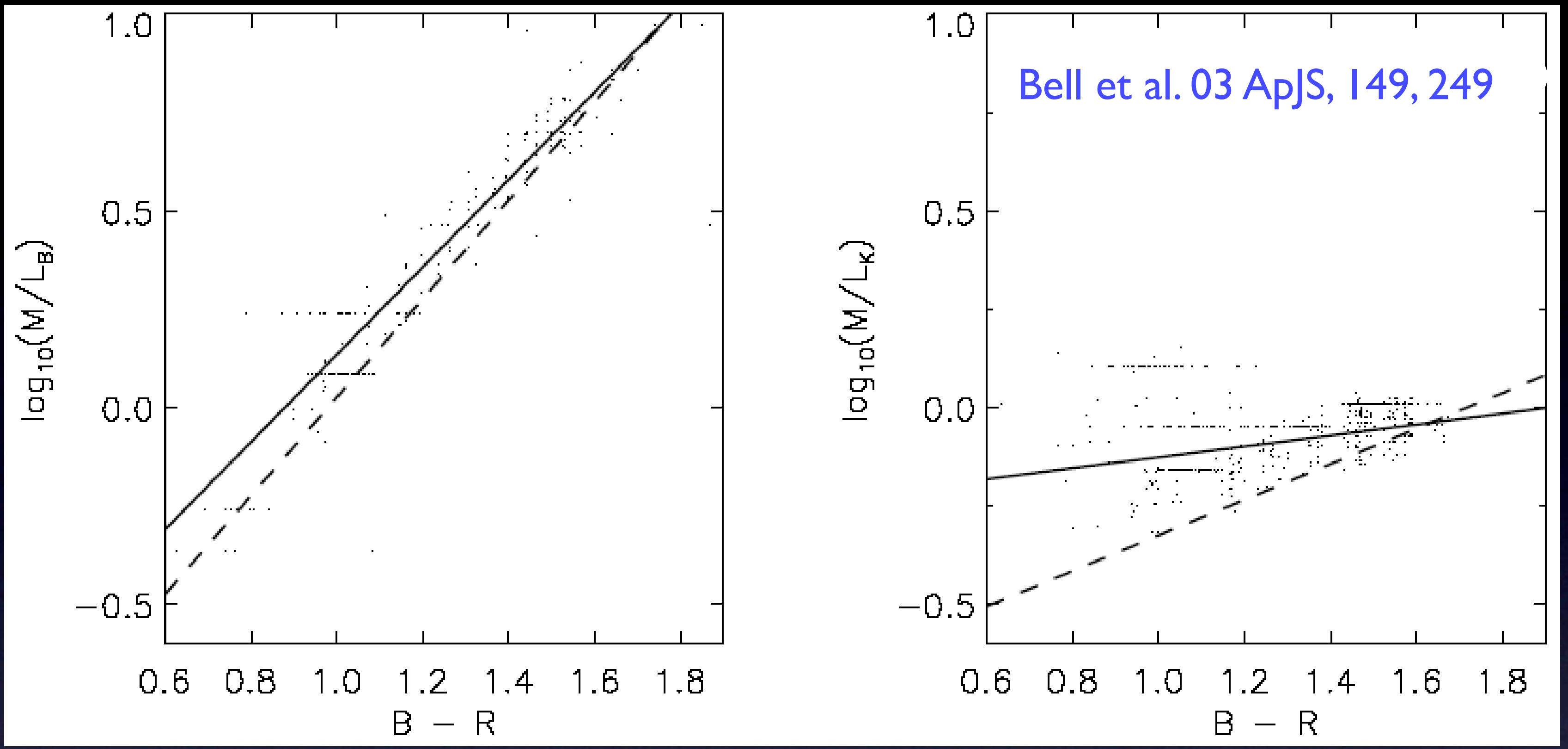

baryon and stellar fractions, a key constraint to the galaxy formation models

NIR bands are ideal for inferring stellar (*and eventually baryonic*) galaxy properties and correlations, (i) to be compared with models, and (ii) to determine the 'efficiency' of galaxy and star formation

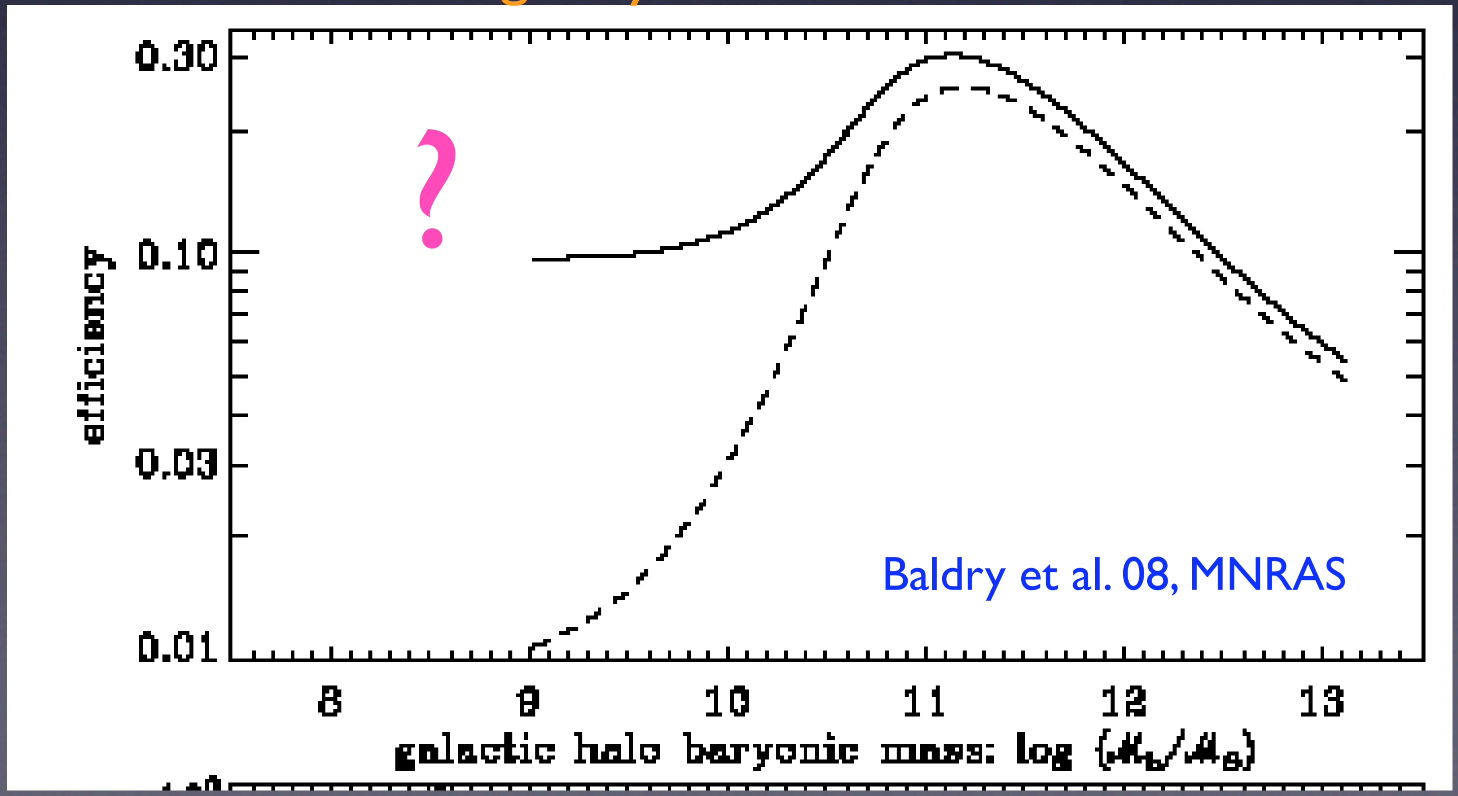

Galaxy L and M_s functions

Table 1. Sample sizes of K-band galaxy luminosity functions.

Paper	Number of galaxies in sample
Loveday (2000)	345
Kochanek et al. (2001)	3878
Cole et al. (2001)	5683
Huang et al. (2003)	1056
Bell et al. (2003)	6282
Eke et al. (2005)	15 644
Jones et al. (2006)	60 869
This work	36 663

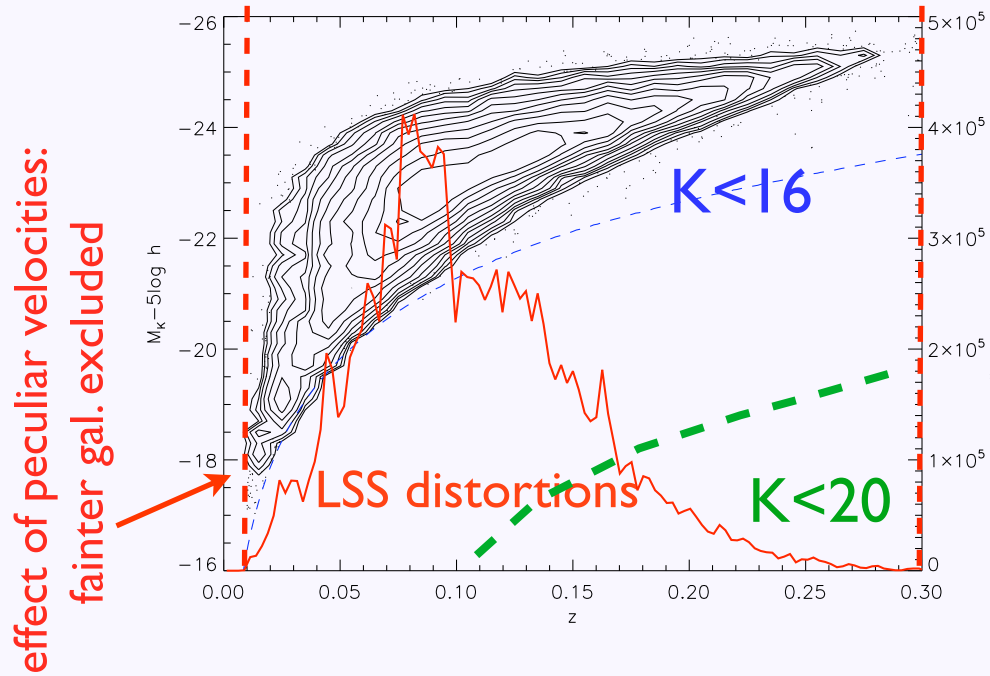

Figure 5. Redshift and K-band absolute magnitude distribution of the sample (contours, points and left-hand y-axis) and histogram of redshift distribution (thick red curve, right-hand y-axis). For reference, the absolute magnitude as a function of redshift corresponding to a source at the K-band faint magnitude limit, with typical K- and evolution-corrections and neglecting the r-band limit, is shown by the blue dashed curve. It can be seen that relatively few galaxies are observed near the K-band magnitude limit; this is because of the r-band magnitude limit.

Luminosity and surface brightness distribution of K-band galaxies from the UKIDSS Large Area Survey

Anthony J. Smith[1⋆], Jon Loveday[1] and Nicholas J. G. Cross[2]

Table 2. Limits set on observed quantities, used to define the sample and to estimate the contribution of each galaxy to the space density.

562.54 deg^2. (up to 4000 deg^2)

Quantity	Minimum	Maximum
K Petrosian magnitude	-	16 mag
r Petrosian magnitude	-	17.6 mag
g fiber magnitude	15 mag	-
i fiber magnitude	14.5 mag	-
K Petrosian radius	-	6 arcsec
$\mu_{e,K}$	-	21 mag arcsec^{-2}
$\mu_{e,r}$	-	24.5 mag arcsec^{-2}
z	0.01	0.3

The K-band LF

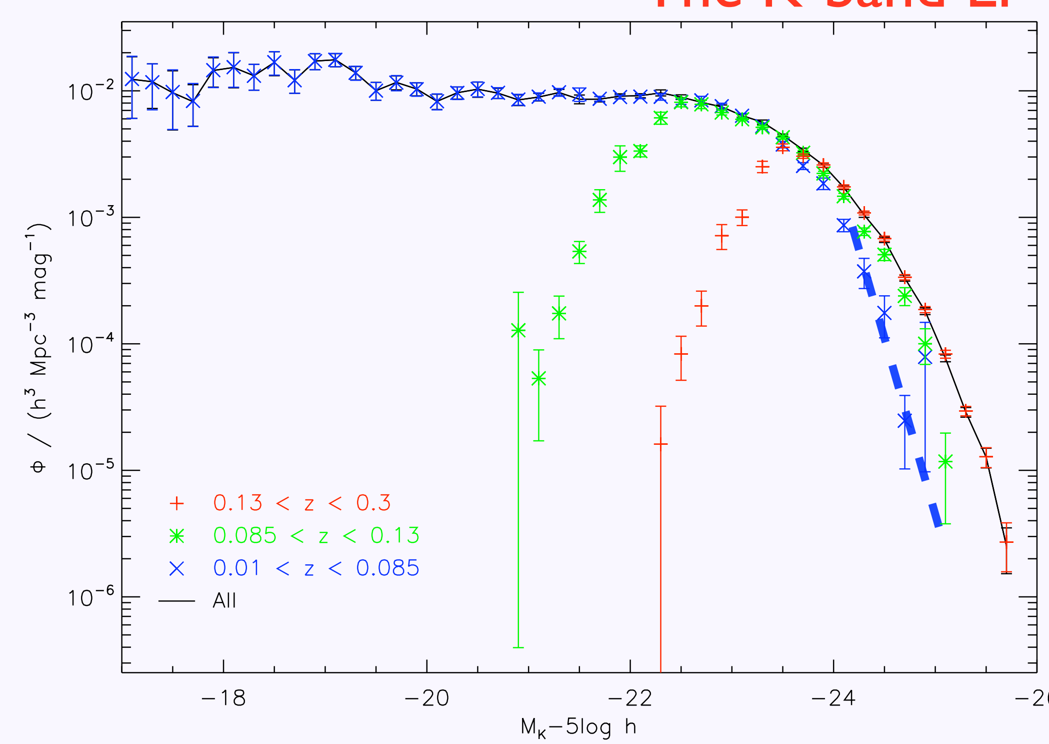

-fainter than K=16, deviates from the Euclidean slope
-sky brightness in K + LAS depth--> r_P<6arcsec (pix. d=24)
-Petrosian K mag and r_P limits--> SB fainter than 20.4m/□"

Galaxy L and M_s functions

Table 1. Sample sizes of K-band galaxy luminosity functions.

Paper	Number of galaxies in sample
Loveday (2000)	345
Kochanek et al. (2001)	3878
Cole et al. (2001)	5683
Huang et al. (2003)	1056
Bell et al. (2003)	6282
Eke et al. (2005)	15 644
Jones et al. (2006)	60 869
This work	36 663

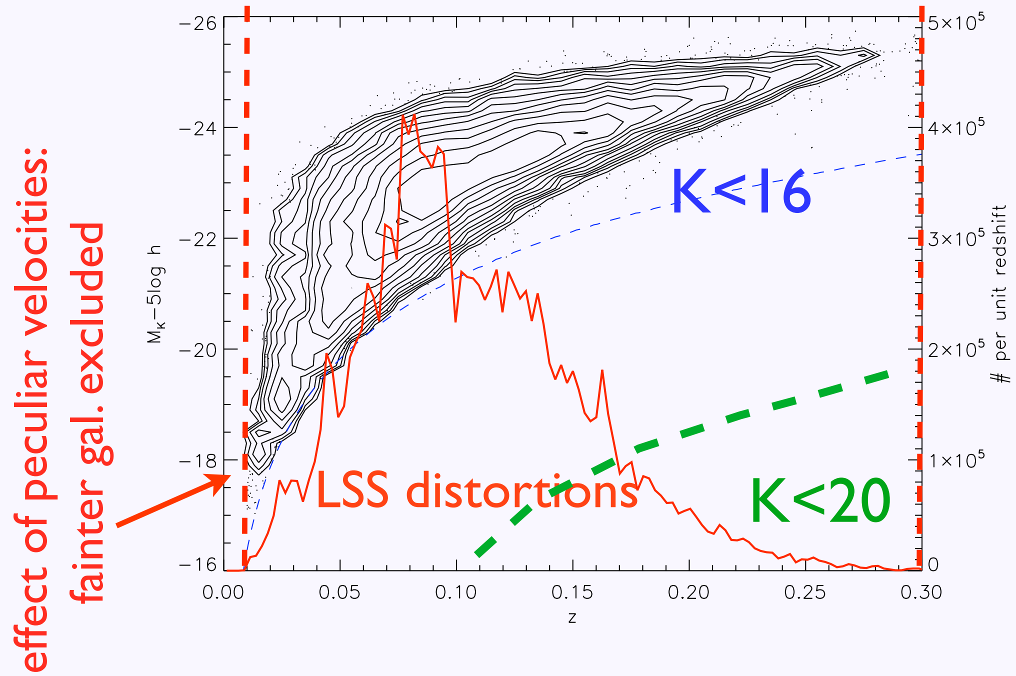

Figure 5. Redshift and K-band absolute magnitude distribution of the sample (contours, points and left-hand y-axis) and histogram of redshift distribution (thick red curve, right-hand y-axis). For reference, the absolute magnitude as a function of redshift corresponding to a source at the K-band faint magnitude limit, with typical K- and evolution-corrections and neglecting the r-band limit, is shown by the blue dashed curve. It can be seen that relatively few galaxies are observed near the K-band magnitude limit; this is because of the r-band magnitude limit.

Luminosity and surface brightness distribution of K-band galaxies from the UKIDSS Large Area Survey

Anthony J. Smith[1⋆], Jon Loveday[1] and Nicholas J. G. Cross[2]

Table 2. Limits set on observed quantities, used to define the sample and to estimate the contribution of each galaxy to the space density.

562.54 deg^2. (up to 4000 deg^2)

Quantity	Minimum	Maximum
K Petrosian magnitude	-	16 mag
r Petrosian magnitude	-	17.6 mag
g fiber magnitude	15 mag	-
i fiber magnitude	14.5 mag	-
K Petrosian radius	-	6 arcsec
$\mu_{e,K}$	-	21 mag arcsec^{-2}
$\mu_{e,r}$	-	24.5 mag arcsec^{-2}
z	0.01	0.3

The K-band LF

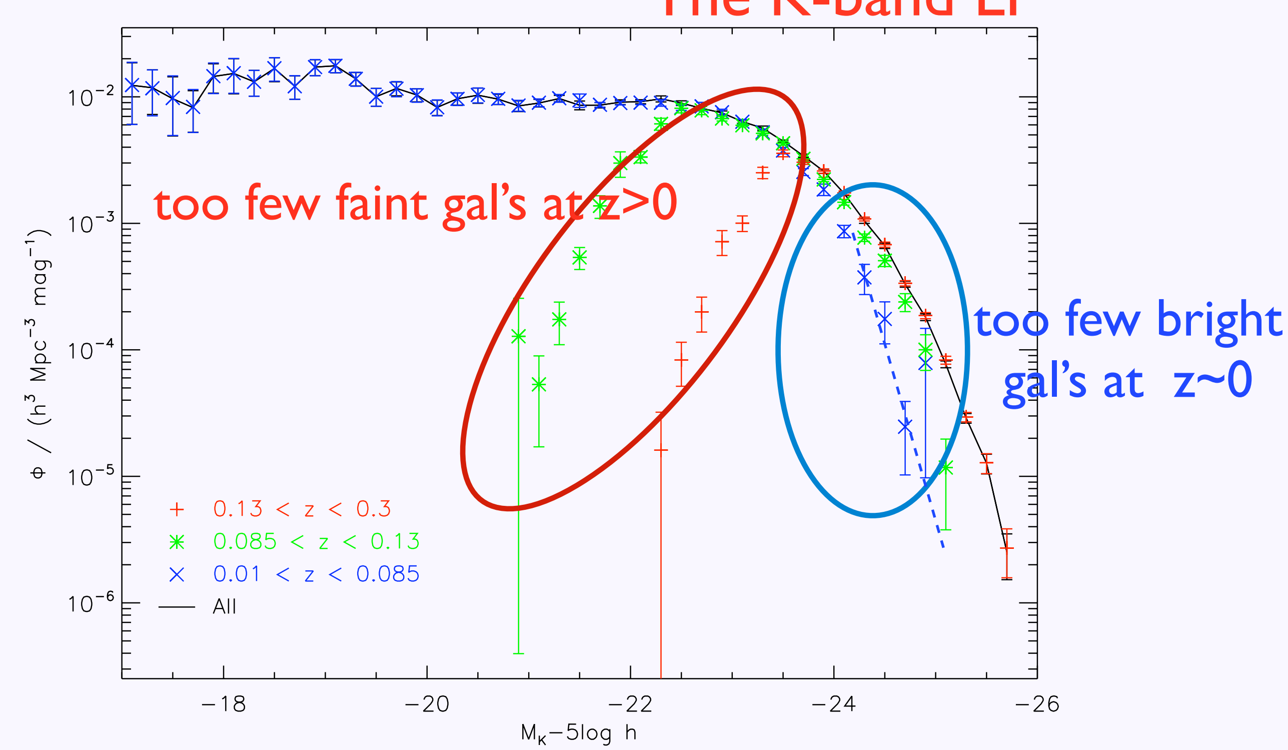

- fainter than K=16, deviates from the Euclidean slope
- sky brightness in K + LAS depth--> r_P<6arcsec (pix. d=24)
- Petrosian K mag and r_P limits--> SB fainter than 20.4m/□"

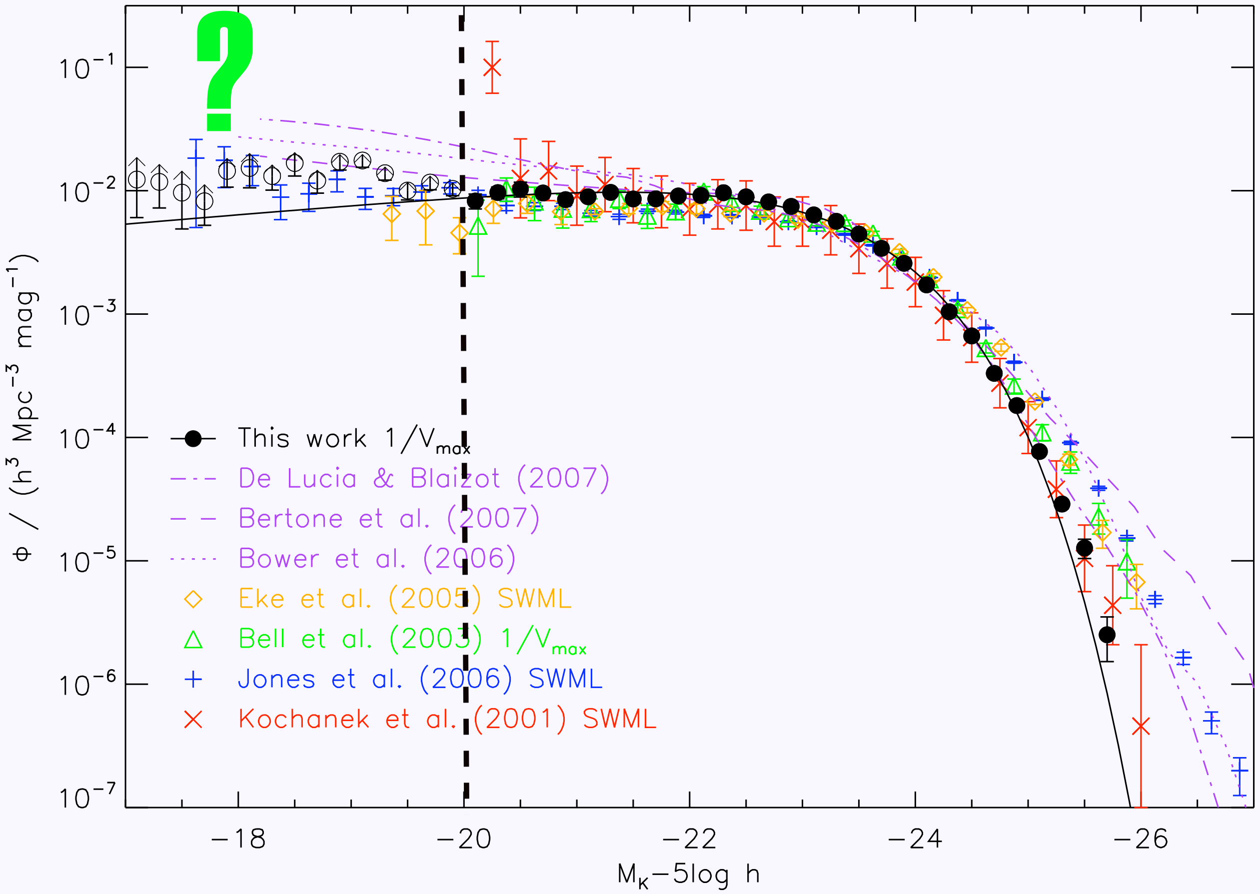

Figure 12. *K*-band luminosity function for the whole sample, with a compendium of published results from observations or semi-analytic models. Only the filled points are used in the Schechter function fit, i.e., $M_K - 5\log h < -20$; the unfilled points are likely to suffer from some incompleteness of low-surface brightness or red, low-luminosity galaxies. Schechter function parameters are $M^* - 5\log h = -23.17 \pm 0.04$, $\alpha = -0.81 \pm 0.04$ and $\phi^* = (0.0176 \pm 0.0009) h^3\,\mathrm{Mpc}^{-3}$.

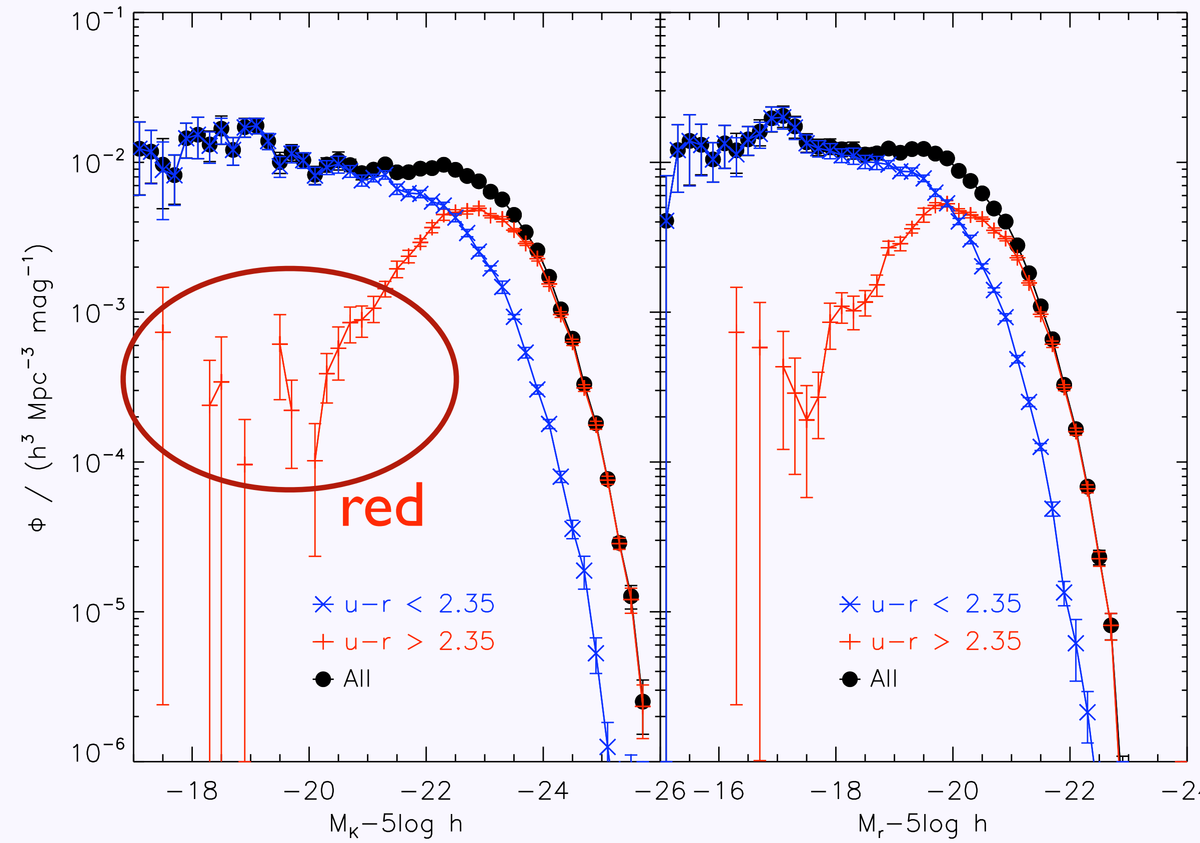

Intrinsic or incompleteness? Detection of red-core low-L gal's is affected by the mag, r, and SB limits

Stellar mass function

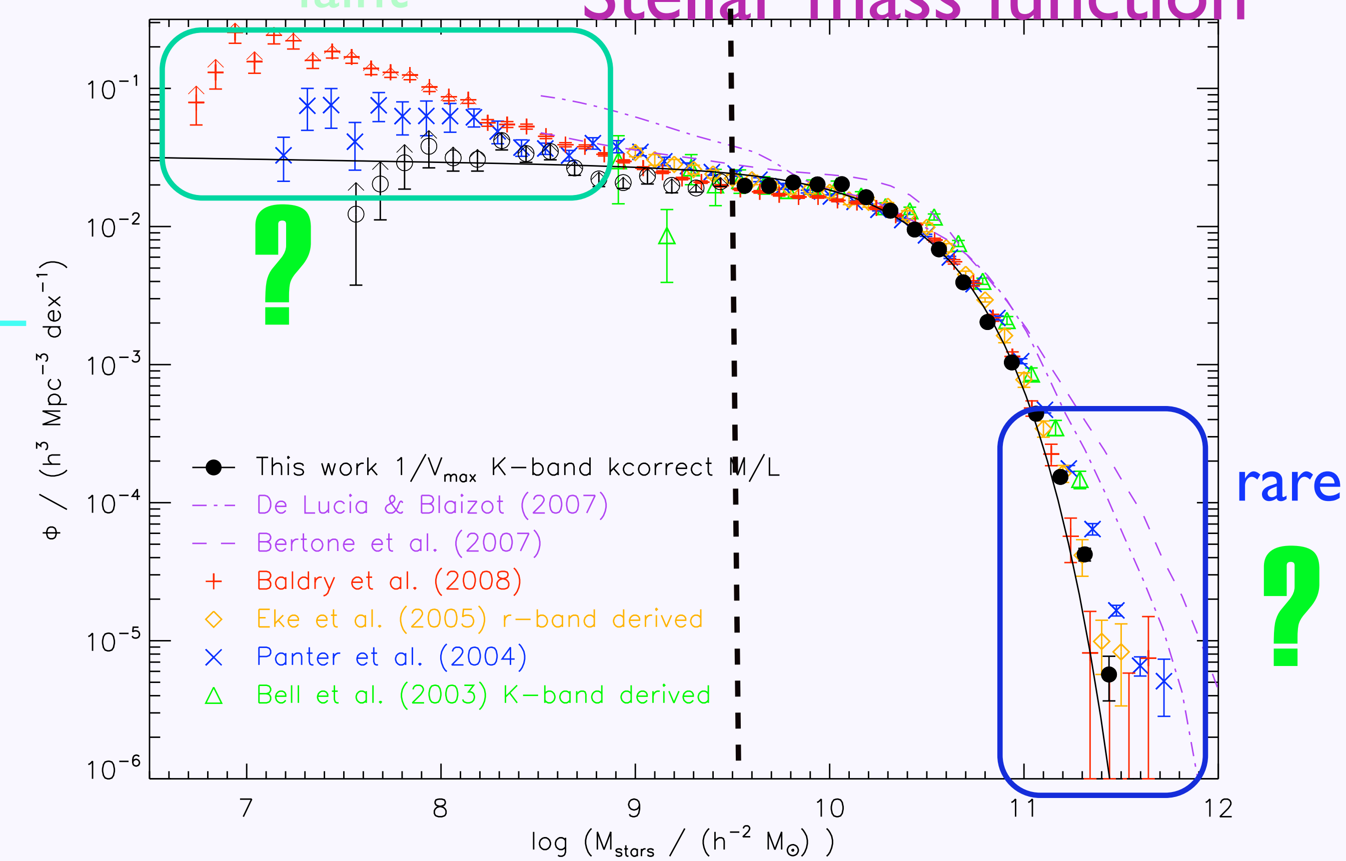

Figure 20. Stellar mass function. Only the filled points are used in the Schechter function fit, i.e., stellar mass greater than $10^{9.5} h^{-2}\,\mathrm{M}_\odot$; the unfilled points are likely to suffer from some incompleteness of low-surface brightness galaxies. Masses calculated from the *K*-band KCORRECT mass-to-light ratios have been increased by 0.1 dex. Schechter function parameters are found to be $\log(\mathcal{M}^* h^2/\mathrm{M}_\odot) = 10.44 \pm 0.02$, $\alpha = -1.02 \pm 0.04$ and $\phi^* = (0.0112 \pm 0.0007) h^3\,\mathrm{Mpc}^{-3}$. Stellar masses based on other

• A NIR survey with both a very large area and high sensitivity (depth of K~21)* will allow to reconstruct the local NIR bivariate L/SB function *(i)* down to the dwarf galaxy pop and including LSB galaxies, *(ii)* with enough statistics for determining accurately the LF bright end (rare gal's) and for *(iii)* allowing to separate the LF function by galaxy types, colors, and environments (*1200 nights for 3E4deg^2 at J=20, K=18.4 in a 4m telescope; UKIDSS-LAS will be for only 4E3deg^2*)

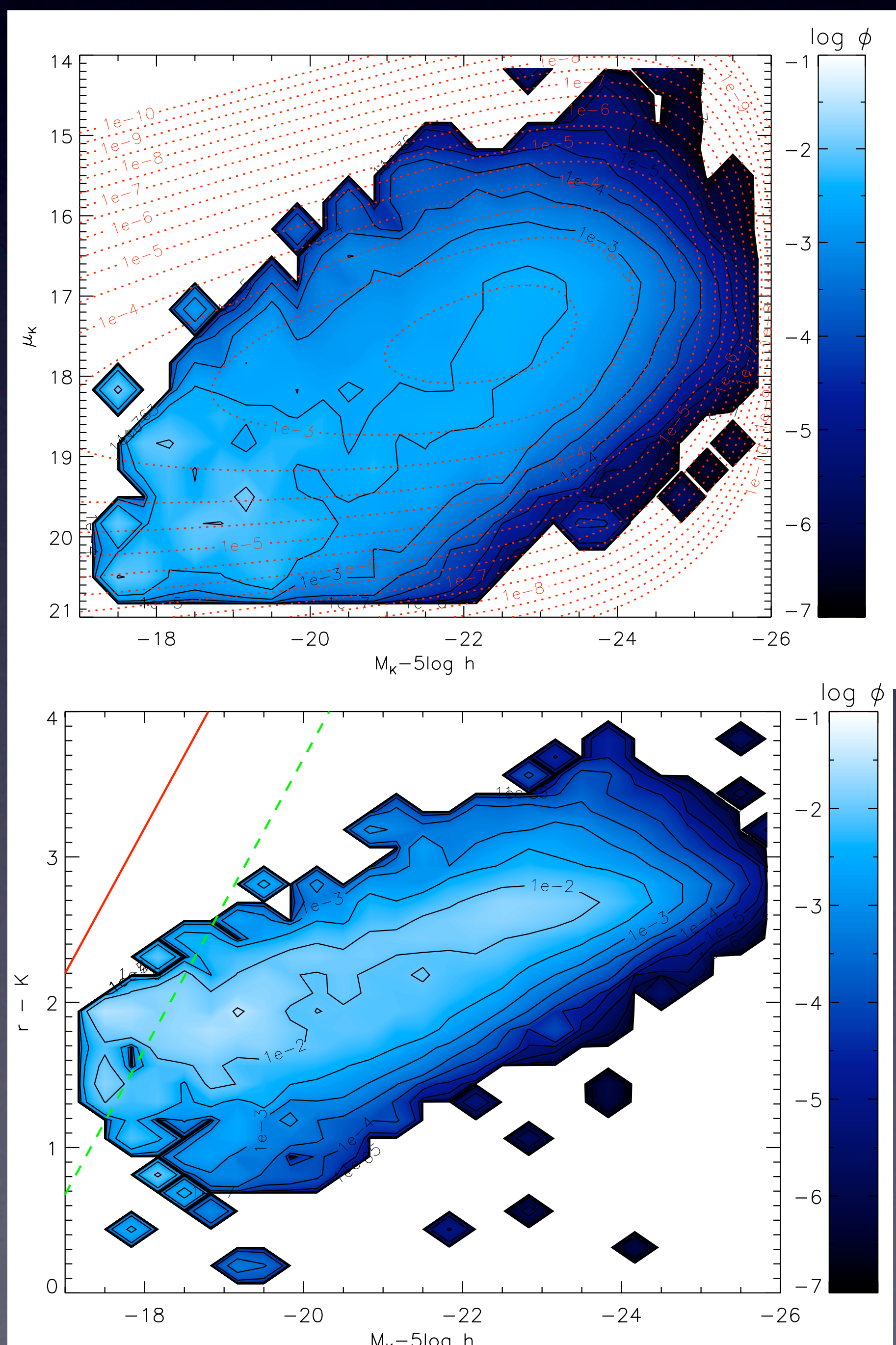

•Redshifts are necessary; for local galaxies (z<0.02), radius is a good discriminant (also *J-K*)

•With at least one optical band, photometric z could be determined; and broad-band colors could be obtained (SP inferences...)

Either add to SASIR *B/g* band or combine information with other deep surveys when possible

(SDSS, Subaru, PanStars, LSST)*

The dwarf galaxy population *(building blocks)*

Property	dIs	BCDs	dEs	dSphs	dS's
M_V (mag) [a]	$\gtrsim -18$	$\gtrsim -18$	$\gtrsim -17$	$\gtrsim -14$	$\gtrsim -18$
μ_{0V} mag/arcsec^2 [b]	$\gtrsim +21$	$\lesssim +19$	$\lesssim +21$	$\lesssim +22$	$\lesssim +23$
r (kpc) [c]	$\lesssim 5$	$\lesssim 5$	$\lesssim 4$	$\lesssim 3$	$\lesssim 5$
H II regions	many	central	none	none	a few
optical appearance	irregular	elliptical	elliptical	elliptical	elliptical
nucleation	none	central	central	very little	central
star formation	low or moderate	starburst	none	none	small
rotation	slow solid-body	solid-body	none	none	slow solid-body
$Z/Z_\odot$ [d]	$\sim 1/40 - 1/3$	$\sim 1/50 - 1/2$	~ 1	~ 1	very low
$M_{HI}/M_\odot$ [e]	$\lesssim 10^9$	$\lesssim 10^9$	$\lesssim 10^8$	$\lesssim 10^5$	$\lesssim 10^9$
$M_{tot}/M_\odot$ [f]	$\lesssim 10^{10}$	$\lesssim 10^{10}$	$\lesssim 10^9$	$\lesssim 10^7$	$\lesssim 10^{10}$
Found mostly in	Field	Field & clusters	Field & clusters	Field & clusters	Field

from Vaduvescu PhD thesis

- What is the abundance and the LF faint-end of different types of dwarf gal's? What is the minimum M_s of galaxies?
- How is the distribution of dwarfs in clusters, groups, filaments and voids?
- How is the stellar structure of dIrr's, BCDs and dS's?

NIR: mass, structure. Deep, LA surveys are necessary to explore dwarfs in the local volume and in different environments.

Some results from Vaduvescu thesis; Vaduvescu, Richer & McCall 06, AJ, 131

SPM observations. Careful photometric analysis. NIR SB profiles: *sech* law.

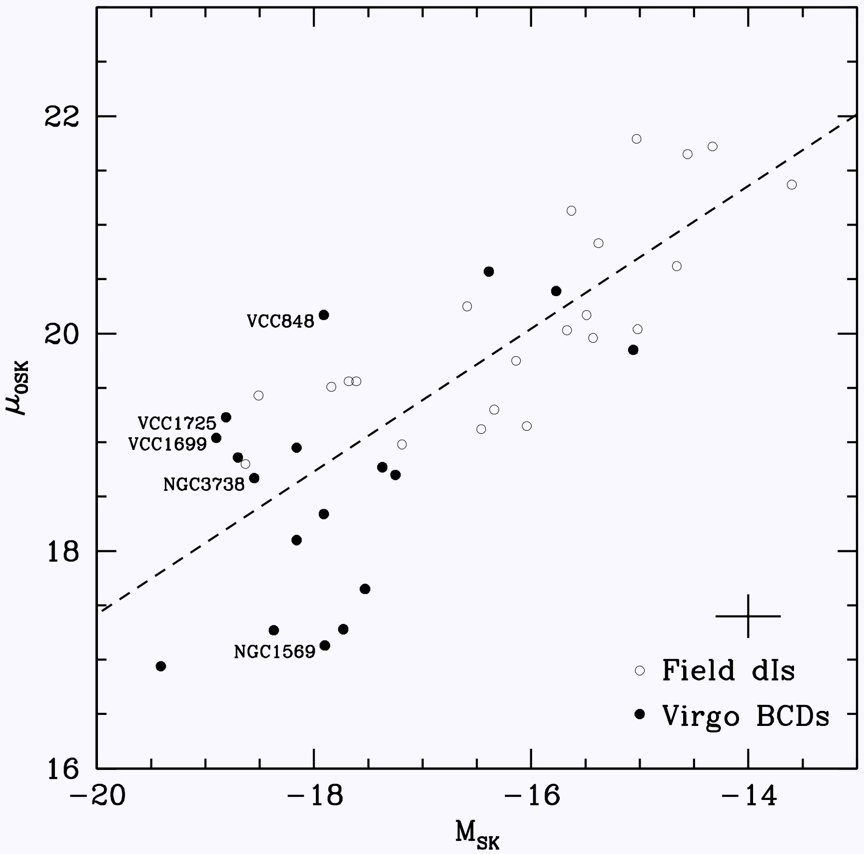

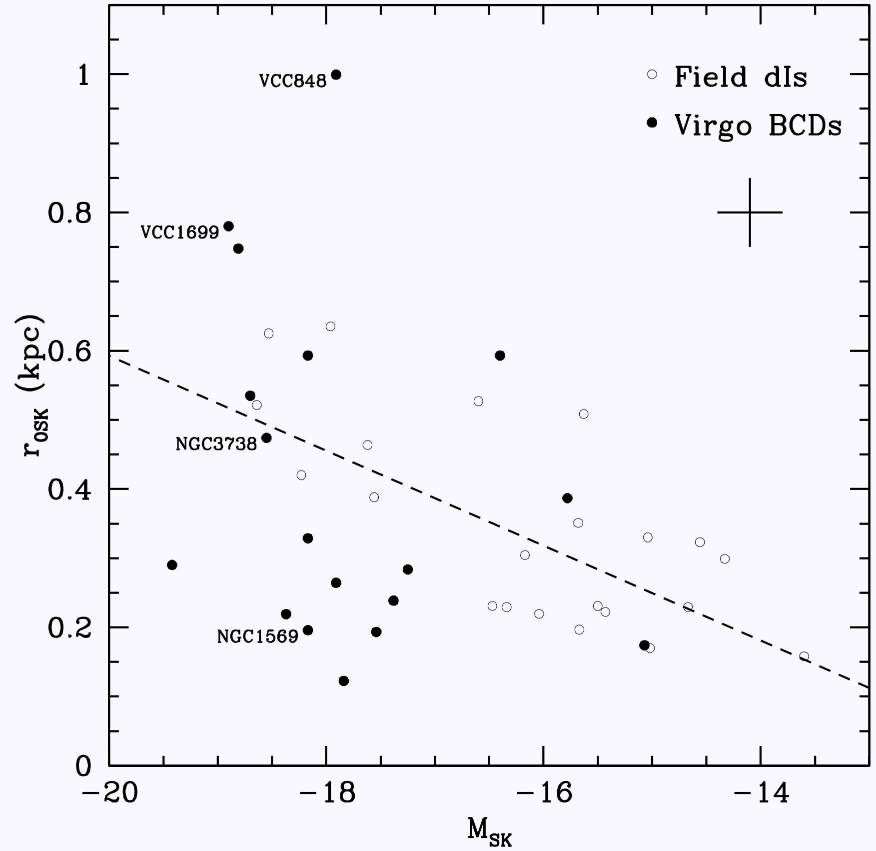

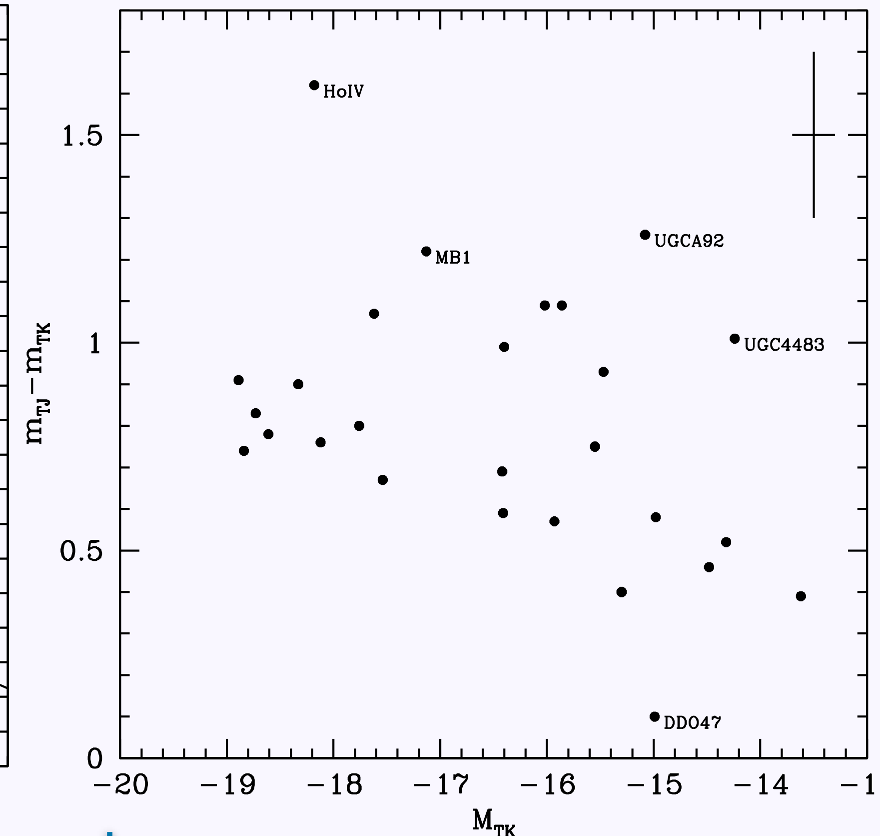

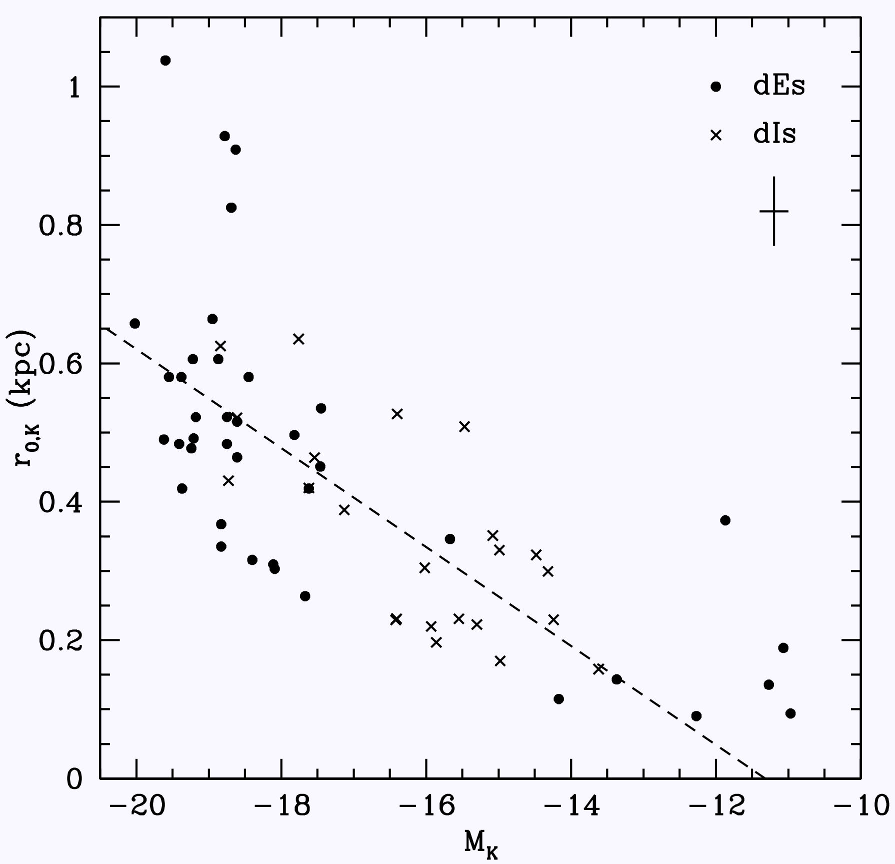

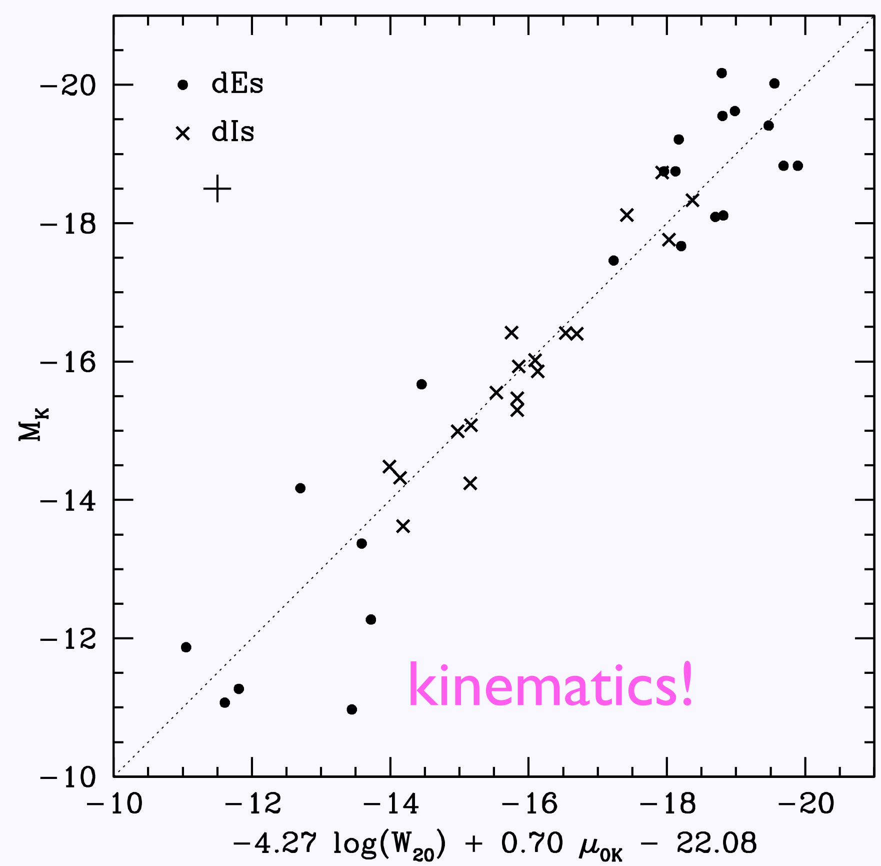

dE and dSph are probably old fossils (or formed by tidal destruction?)

What about dIrr, BCD, dS?
BCD are dIrr in bursting phase and dE are fading dIrr?

Key constraints to the LCDM model (*see Valenzuela's talk*)

Baryonic quantities, *the ultimate goal*

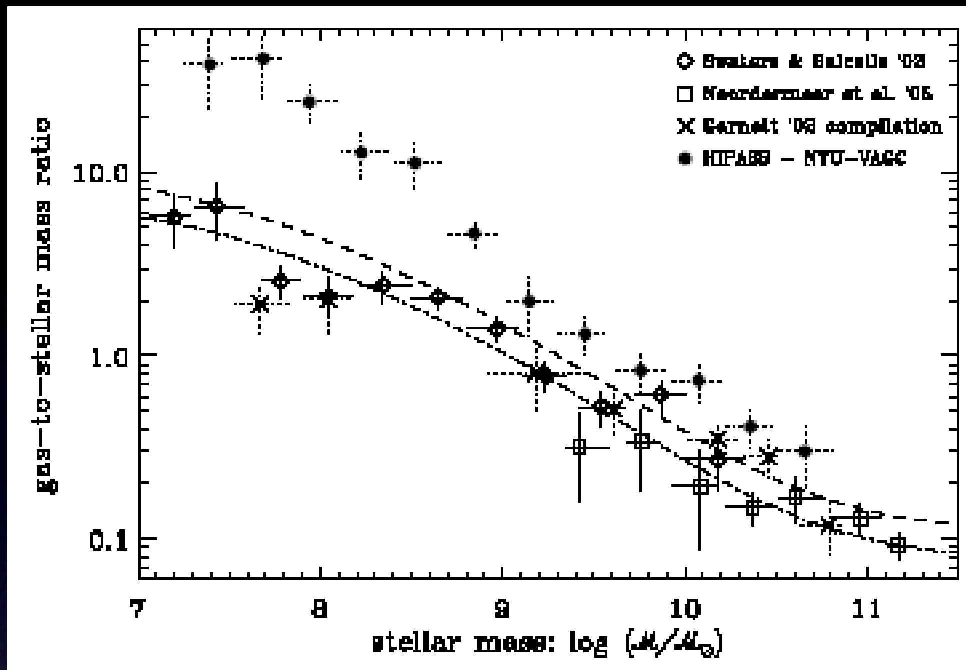

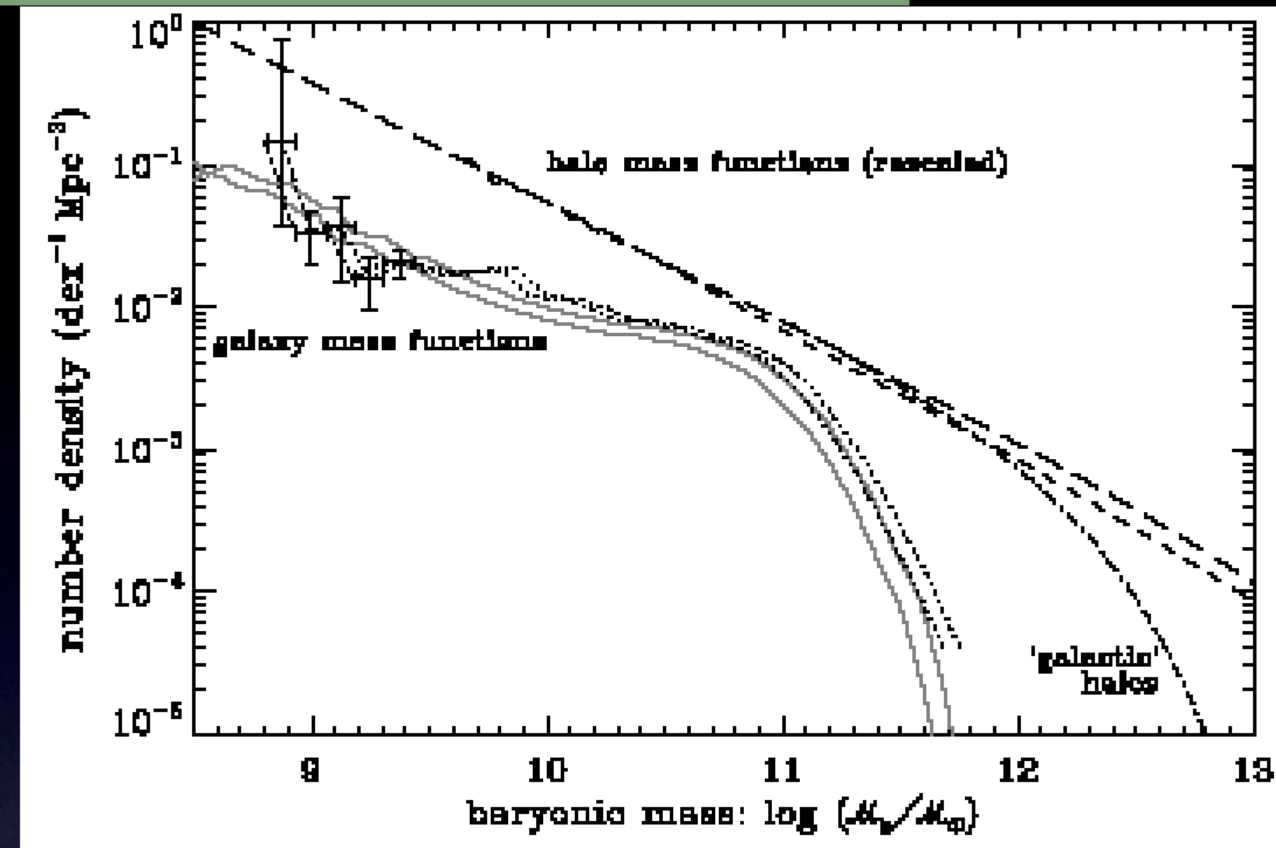

To fully understand galaxy formation & evolution, we need to constrain stars, gas, and dust

Baryonic Tully–Fisher relation for extremely low mass Galaxies

Ayesha Begum,[1★] Jayaram N. Chengalur,[2] I. D. Karachentsev[3] and M. E. Sharina[3]

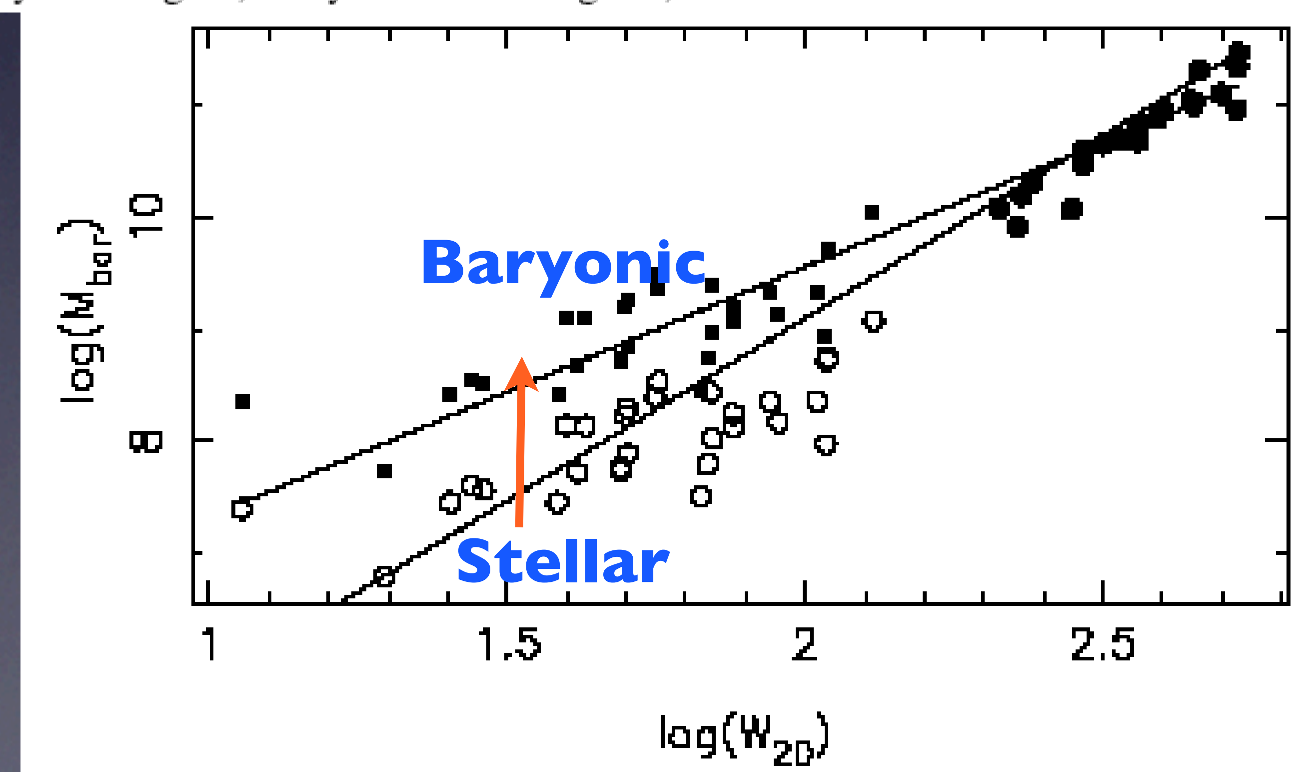

Synergy of NIR surveys with HI surveys --> the real mass backbone of galaxies

Disk galaxy scaling relations

Avila-Reese, Zavala, Firmani, Hernandez-Toledo, AJ, in press; (Zavala, A-R, H-T, Firmani 03, A&A)

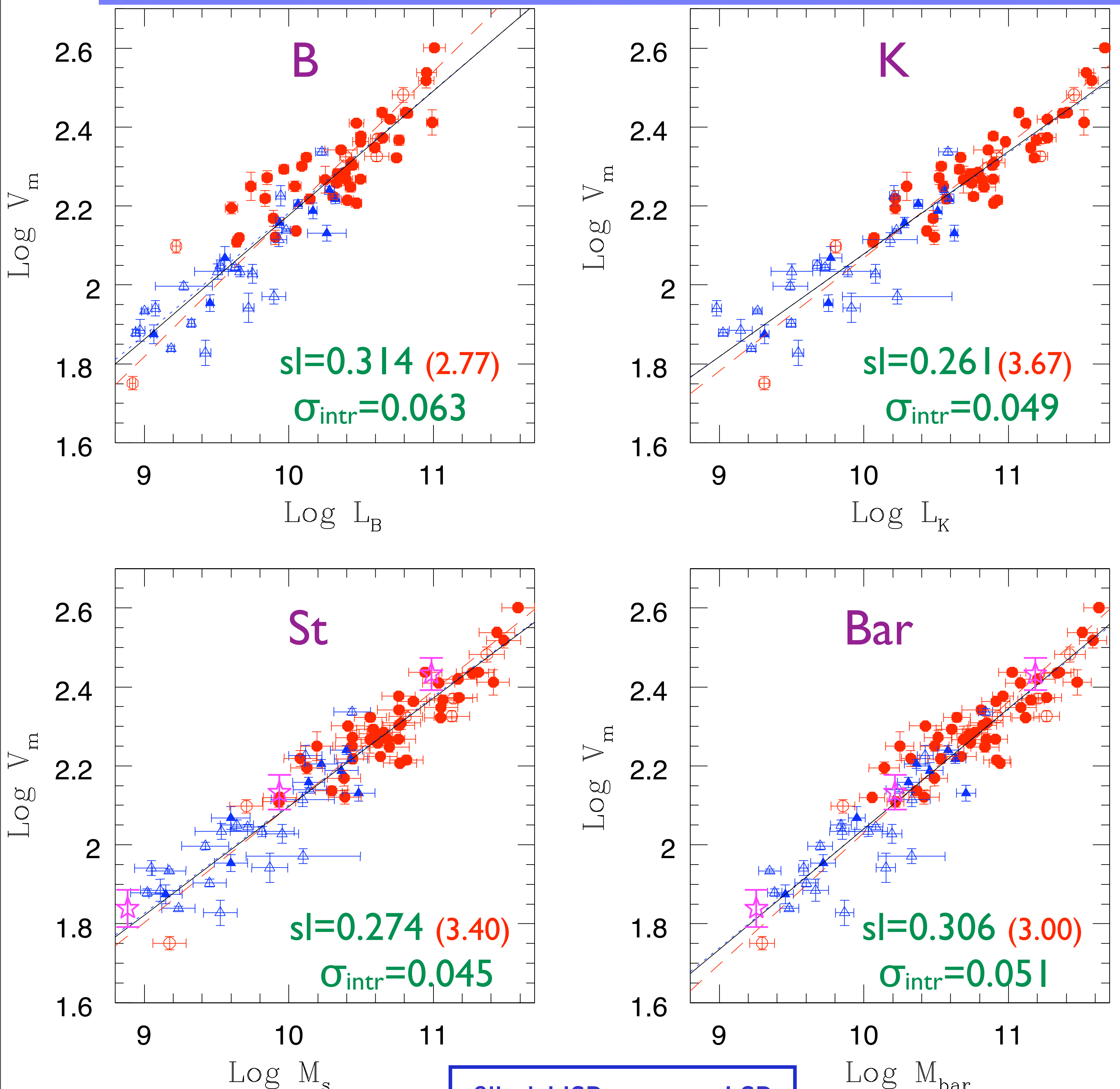

filled: HSB empty: LSB
○: red Δ: blue

Very reduced number of 'useful' galaxies

The TF relations

- The bar TFR is steeper than the st one.
- Intrinsic scatters: change from bar to st and to K-band cases
- Crucial for constraining models

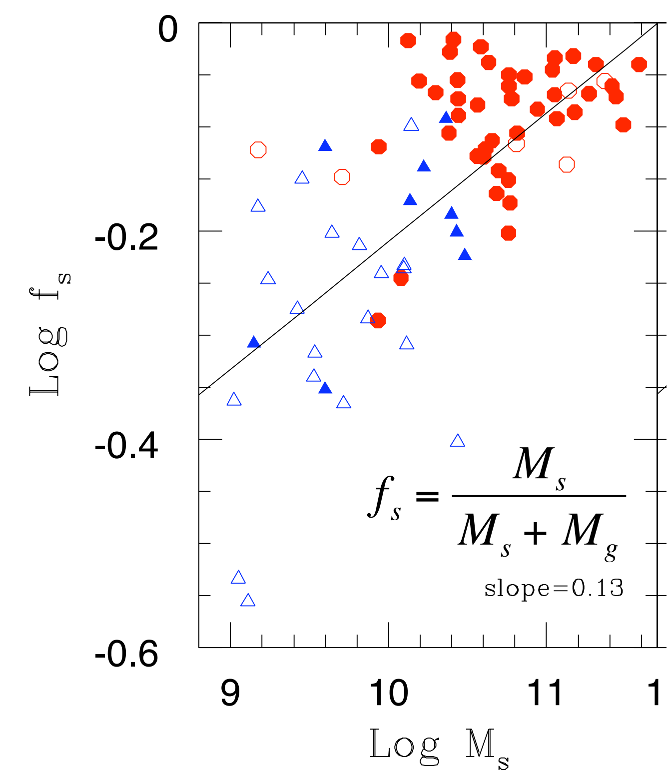

$$f_s = \frac{M_s}{M_s + M_g}$$

$$f_{\rm s} = 0.65 (M_{\rm s}/10^{10} {\rm M}_\odot)^{0.13}$$

?

The radius-*M* (-*L*) relations

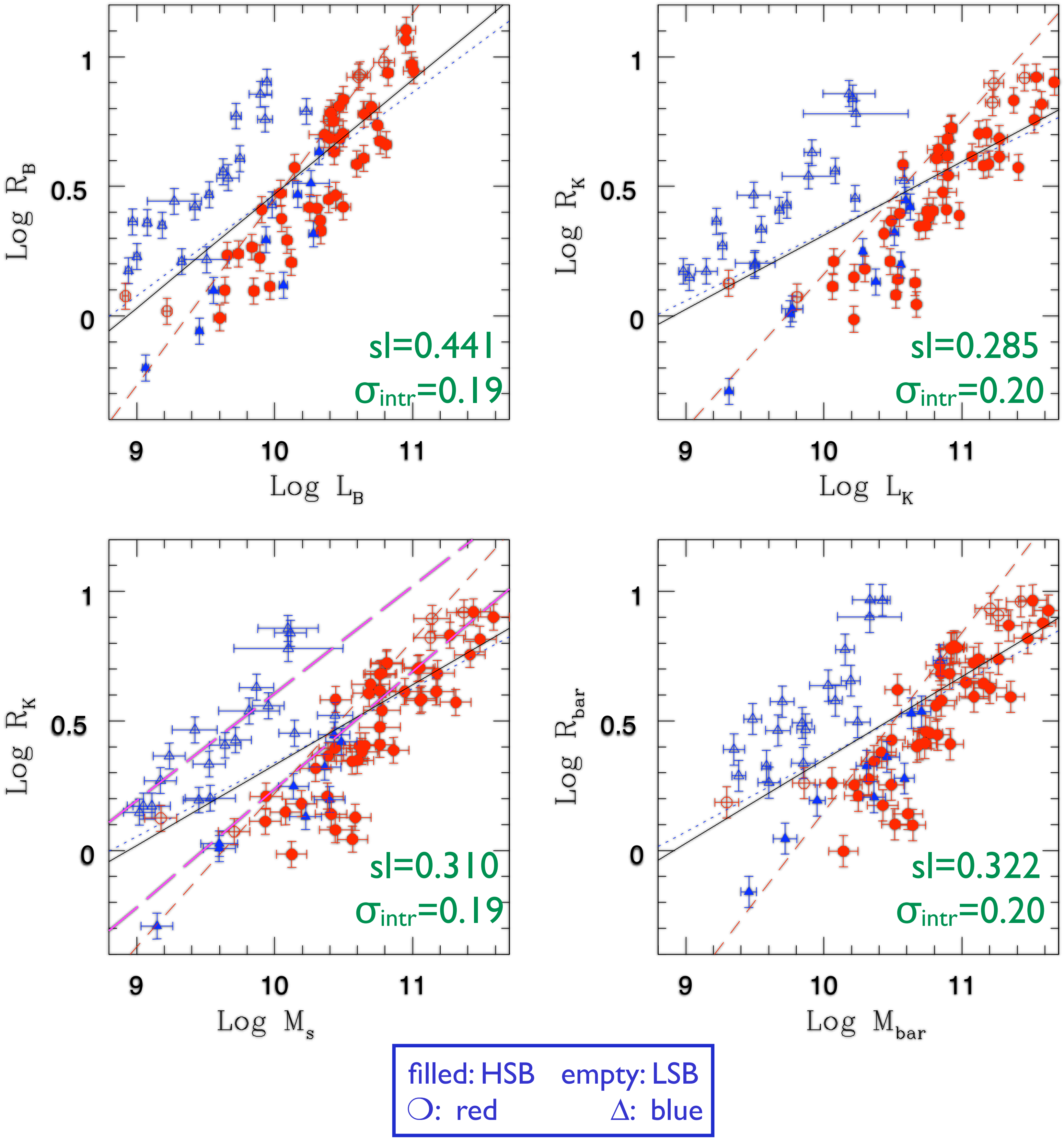

- Scattered and segregated by SB, and less by color

- Slopes around 0.3, but for the *B* band case, 0.44. ☛

A wide range in SB is crucial for this relation. Most of previous similar samples did not include LSB gal's

Scaling relations are fossils of: cosmological initial conditions + gal. evolution + SP evolution. Observational constraints (including early-types) are yet very limited. Even scatters are highly informative

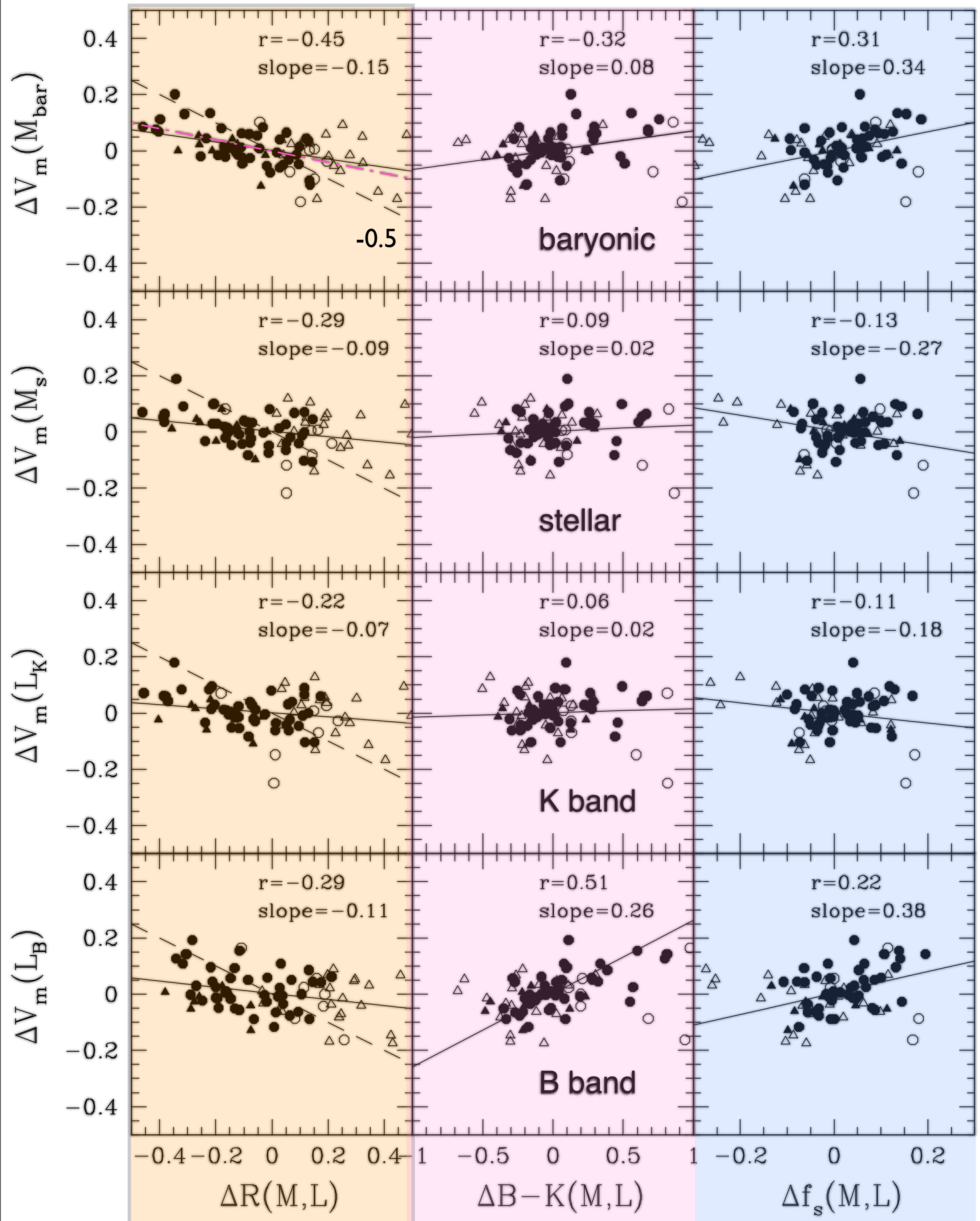

Trends among the residuals

✤In the bar case there is a (weak) anti-correlation: *sl=-0.15*. The level of dependence of V_m on the disk surface density decreases as SB decreases (the halo becomes dominant). Could MOND explain this?

✤The anti-corr'n disappears in the st and *L* cases. *Why? (A SF effect)*

✤The *B*-band TFR residuals increase as the gal's are deviated to the redder side (Kannappan+ 02). For a given L_K, the bluer the color, the larger L_B.

✤The bar TFR residuals are larger for gal's that end with higher st. fractions (formed earlier and/or had an efficient SF)

The scaling rel's change for luminous, stellar, and baryonic quantities: clues to models of gal. formation and cosmology

The stellar structure of galaxies in the NIR

•NIR morphology is different to the optical ones *(de Blok, Puerari,...)*: morphological reclassification. B/D ratio and dust corrections

•NIR bar and bulge statistics (z~0 and z>0 and as a function of environment): secular evolution of galaxies & dynamical history *(Hernandez-Toledo+)*

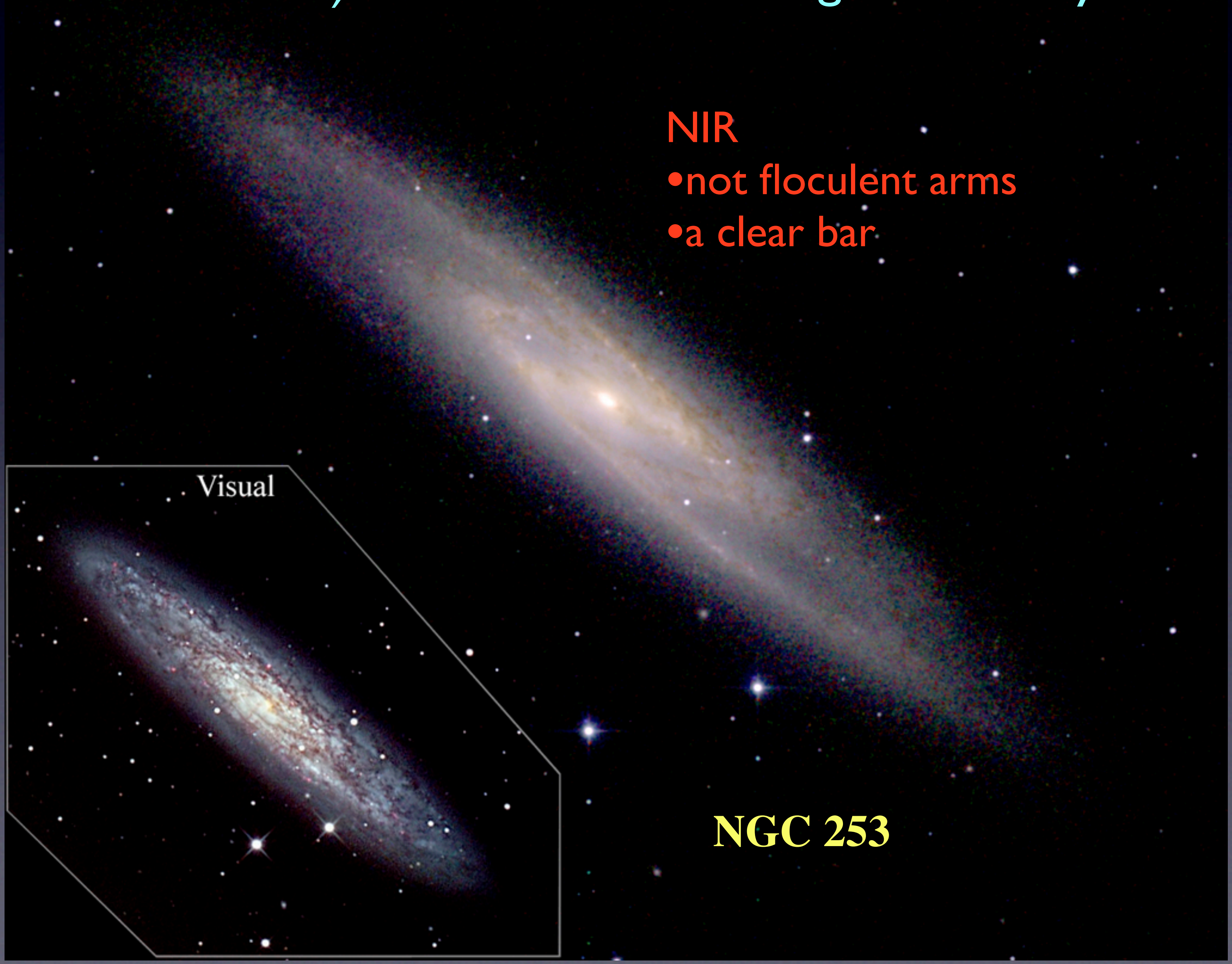

•NIR *CAS* parameters & lopsideness statistics: galaxy assembly history, dark matter halo structure and sub-structure, etc. *(Hernandez-Toledo+, Valenzuela+)*

•Outer stellar disks structure -cutoff?, warps

•Color gradients: inside out formation, secular mass redistribution, dust gradient?

•LSB galaxy stellar structure

Physical interpretation of the near-infrared colours of low-redshift galaxies

MNRAS, 384,930

C. Eminian,[1★] G. Kauffmann,[2] S. Charlot,[3] V. Wild,[2] G. Bruzual,[4] A. Rettura[5] and J. Loveday[1]

Colours of SF-ing galaxies are poorly understood.
5800 SDSS/UKIDSS late-type local galaxies

- -More strongly SF-ing galaxies have redder H-K color.
- -The more dust attenuation, the redder H-K
- -TP-AGB stars dominate the H & K bands following a SF burst.
- -TP-AGB stars are the main source of dust in nuclear region of the galaxy

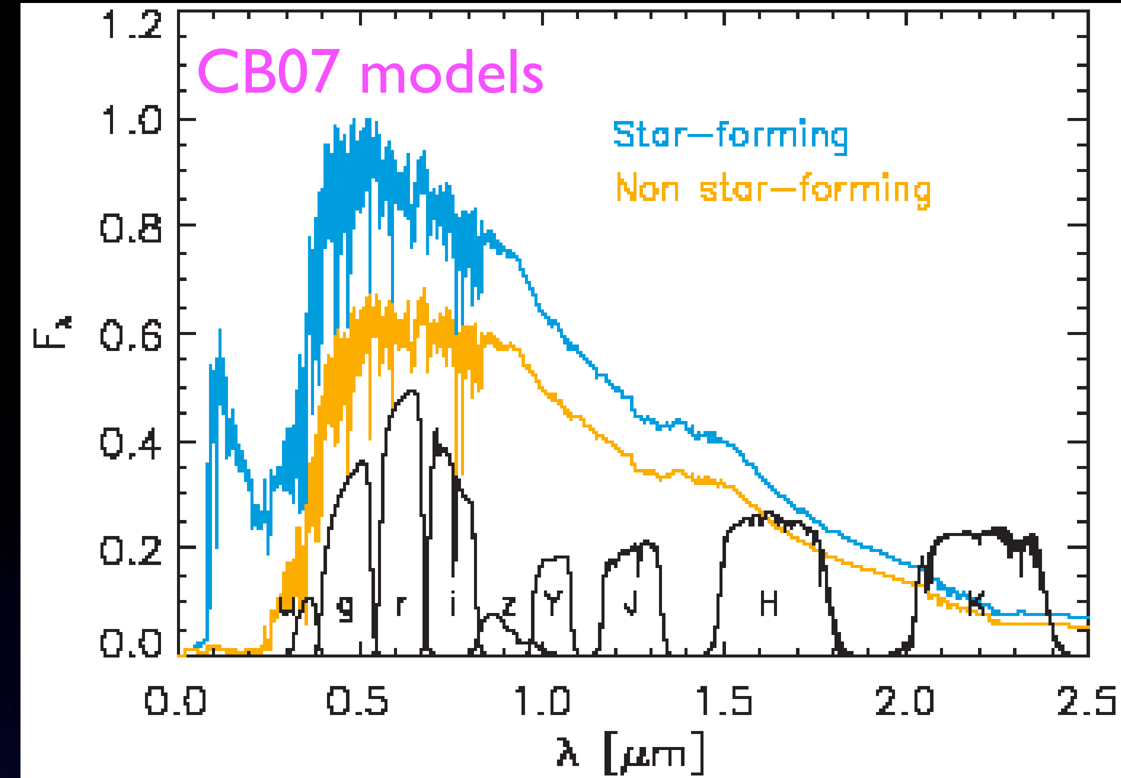

non-SFing

Colour	Age	$Z_{\rm stellar}$	A_z	b/a
	Correlation coefficient			
$g-r$	0.4 ± 0.1	0.05 ± 0.08	-0.02 ± 0.05	-0.08 ± 0.11
$i-z$	0.20 ± 0.09	0.00 ± 0.07	0.16 ± 0.05	-0.08 ± 0.05
$Y-J$	0.08 ± 0.04	0.04 ± 0.04	0.02 ± 0.02	-0.04 ± 0.02
$H-K$	-0.04 ± 0.04	0.07 ± 0.04	0.14 ± 0.03	-0.01 ± 0.03

SFing

Colour	SFR/M*	Age	$Z_{\rm gas}$	Hα/Hβ	A_z	b/a
			Correlation coefficient			
$g-r$	-0.49 ± 0.05	0.62 ± 0.09	0.09 ± 0.05	0.11 ± 0.03	-0.09 ± 0.03	-0.34 ± 0.04
$i-z$	-0.37 ± 0.05	0.46 ± 0.08	0.06 ± 0.05	0.13 ± 0.03	-0.04 ± 0.04	-0.31 ± 0.04
$Y-J$	-0.02 ± 0.02	0.07 ± 0.05	0.08 ± 0.03	0.20 ± 0.03	0.12 ± 0.03	-0.20 ± 0.02
$H-K$	0.23 ± 0.03	-0.17 ± 0.05	0.03 ± 0.03	0.25 ± 0.03	0.23 ± 0.04	-0.12 ± 0.03

-Models: g-r vs Y-K could break the age-Z degeneracy.

-Data: marginally. Y-K is metal sensitive (see also Galay+02)

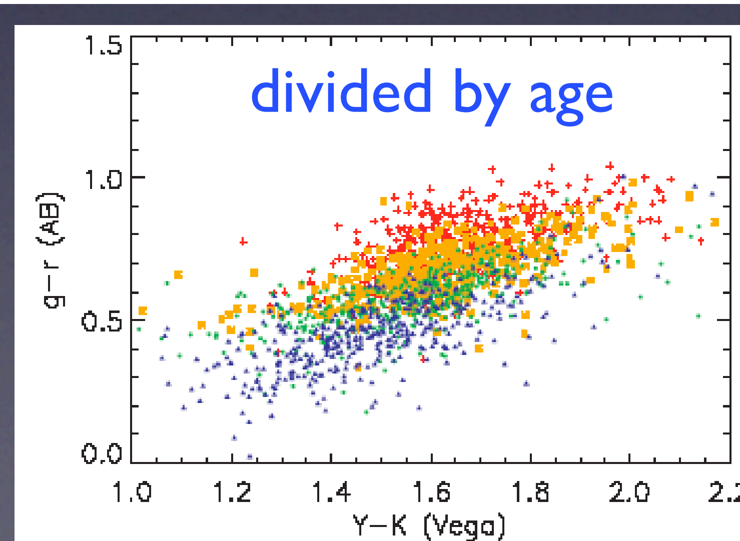

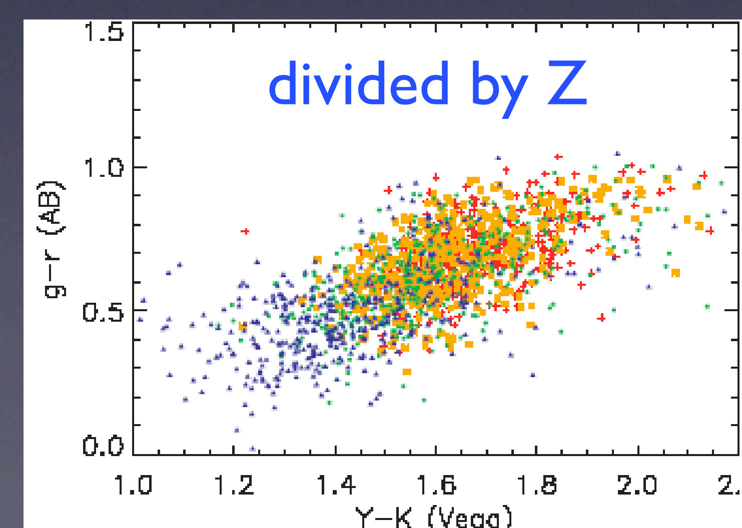

NIR photometry is very useful for understanding the physics of interacting galaxies *(several of their underlaying properties are distorted in optical bands)*: a deep and extensive NIR catalogue of these galaxies is desirable

NIR colors as probes of interacting galaxies

(Geller et al. 06, AJ, 132, 2243)

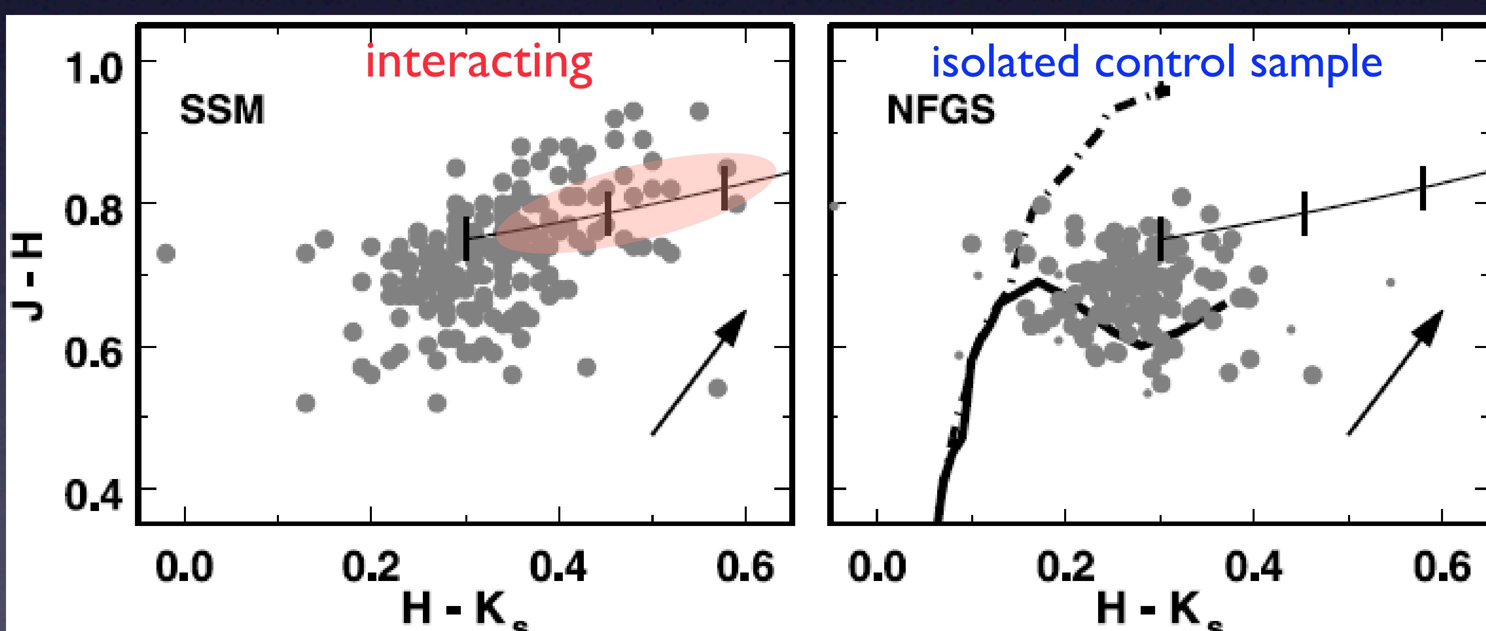

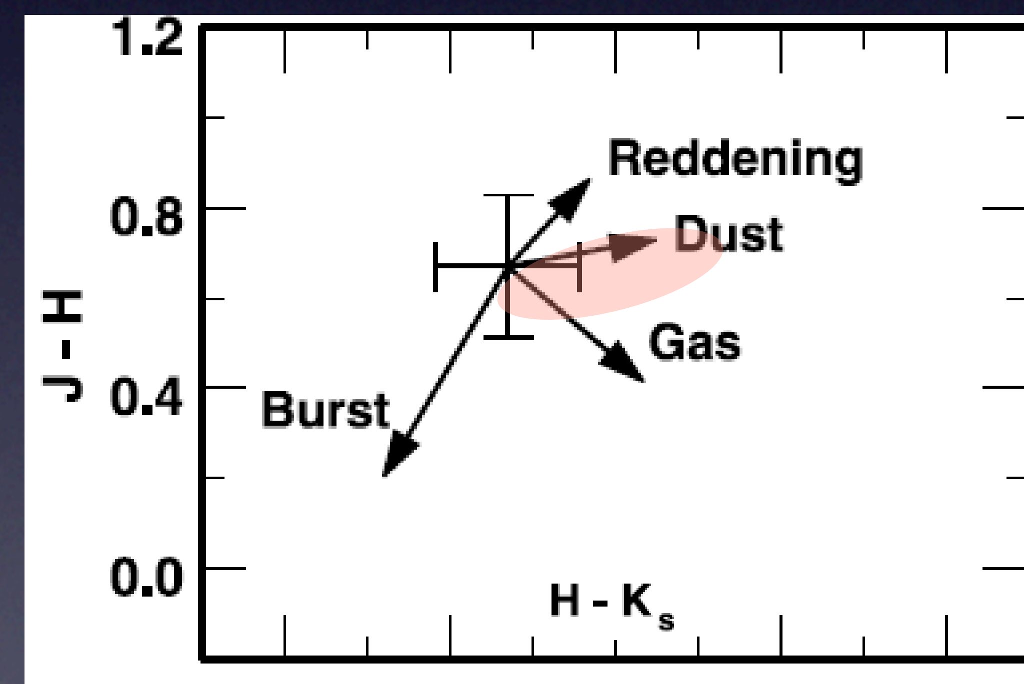

$H - K$. In the color-color diagram the reddest objects in $H - K$ are also red in $J - H$. The colors of these objects follow a track for thermal emission from 600–1000 K dust. The reddest $H - K$ colors require emission from hot dust.

Hot dust could be a new tracer of SF in compact dust-enshrouded bursts. The z=0 SFRD could be underestimated

The z>0 universe

A large area survey of well-defined mass-tracing objects (e.g., galaxies in the NIR) in a given z-range is useful for several LSS and structure formation problems.

--Baryonic Acoustic Oscillations (e.g. SDSS-III): d_A at z=0.3, 0.6 & 2.5

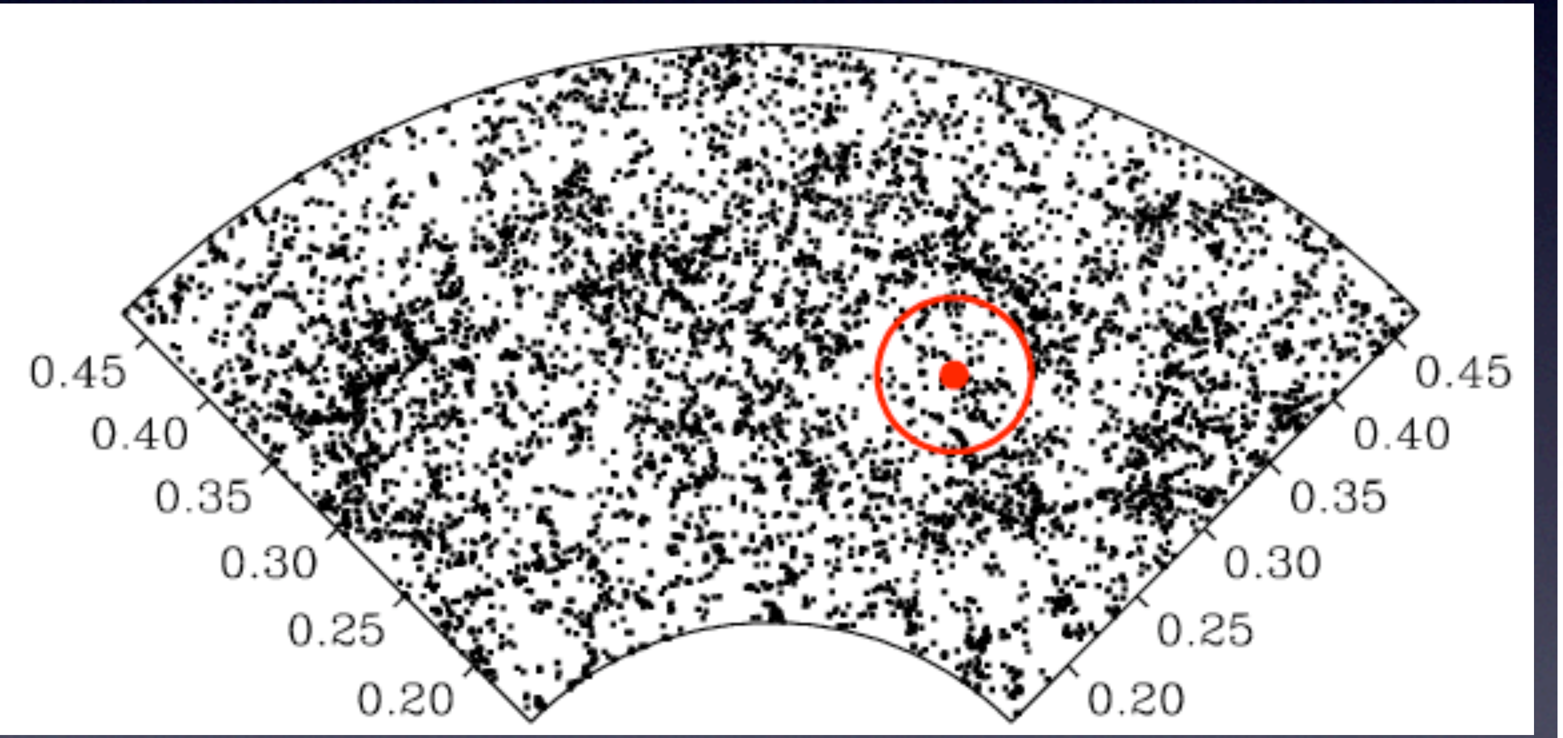

~150 Mpc, z=0.3

Used to measure dark energy properties

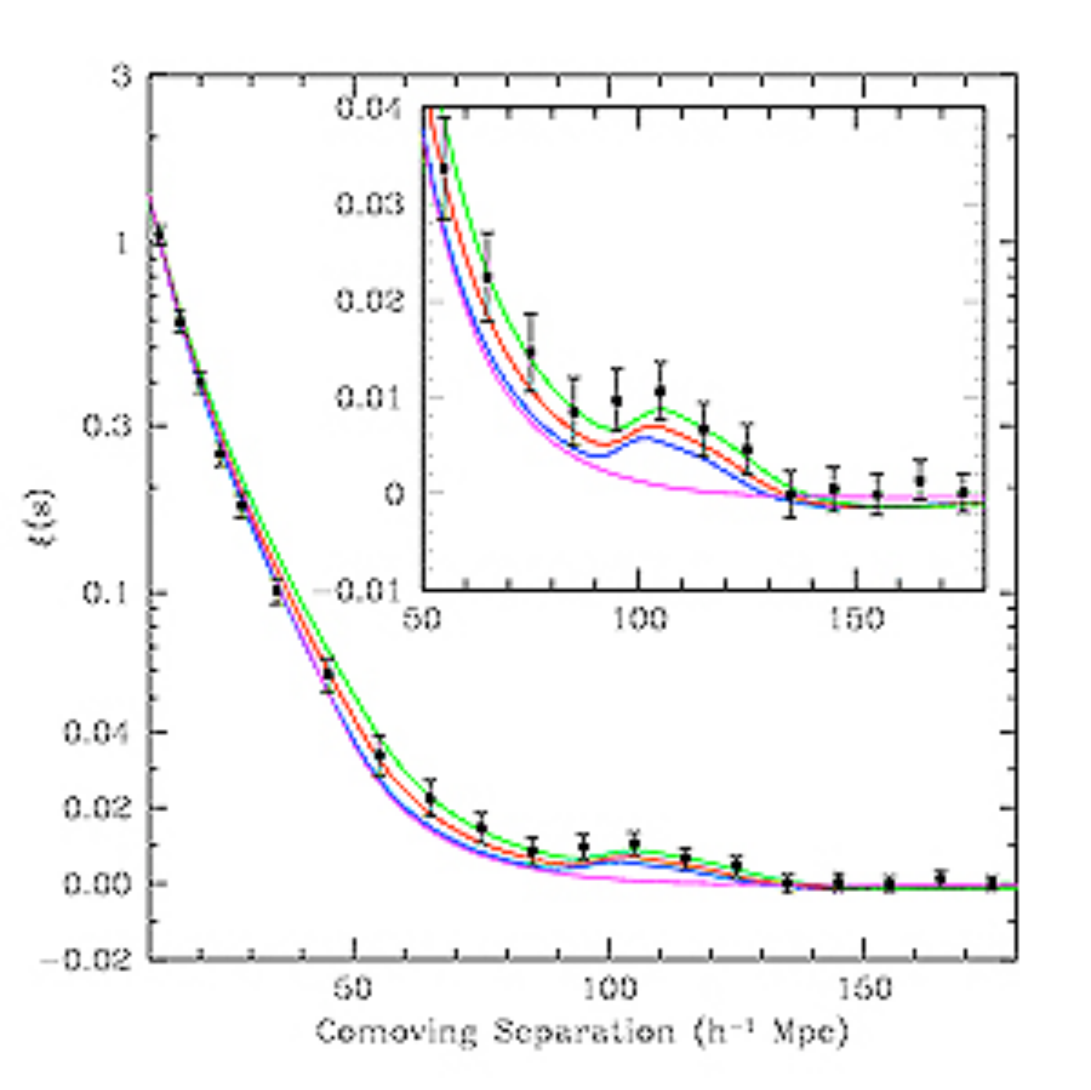

Imprint of superstructures in the CMBR due to the ‘late-time’ Integrated Sach-Wolfe (ISW) effect

$$(\Delta T/T)|_{\rm ISW} = -2\int \dot{\Phi}\, d\eta,$$

$$\Delta\Phi \sim \frac{4\pi G}{3} r_c^2 \rho_c \delta(\Delta z)$$

depends on DE

Accelerated expansion due to dark energy (z<1) causes even gentle large-scale potential wells and hills to decay over the time it takes a photon to travel through them--> gravitational z--> secondary anysotropies in the CMBR: cross-correlate with LSS at the z of the effect.

Rudnick+07ApJ, 671

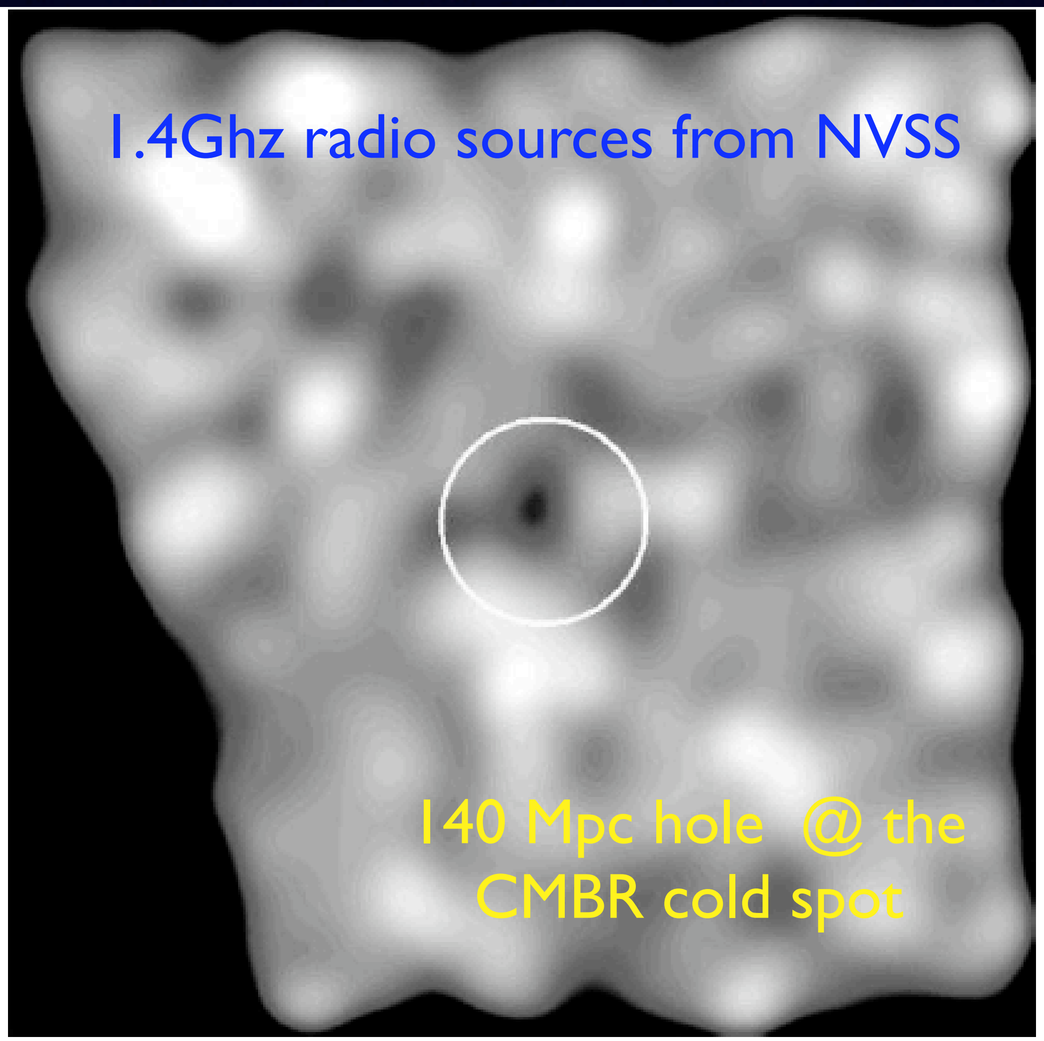

Fig. 1.—50° field from smoothed NVSS at 3.4° resolution, centered at $l = 209°$, $b = -57°$. Values range from 9.3 mJy beam^{-1} (*black*) to 21.5 mJy beam^{-1} (*white*). A 10° diameter circle indicates the position and size of the *WMAP* cold spot.

The ISW signal peaks at l~20 and z=0.5: superstructures of ~4deg or 100 Mpc/h

Granett+ 0805.3695 (LRG in SDSS)

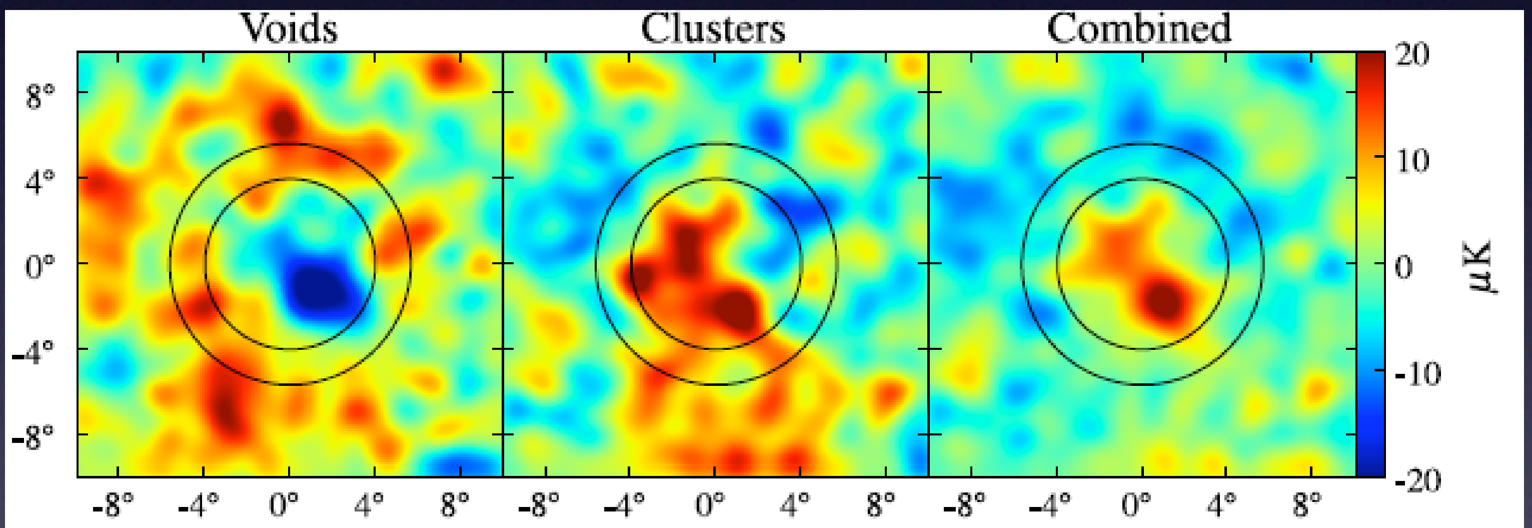

Fig. 1.— Stacked regions on the CMB corresponding to supervoid and supercluster structures identified in the SDSS LRG catalog. We averaged CMB cut-outs around 50 supervoids (left) and 50 superclusters (center), and the combined sample (right). The cut-outs are rotated, to align each structure's major axis with the vertical direction. Our statistical analysis uses the raw images, but for this figure we smooth them with a Gaussian kernel with FWHM 1.4°. Hot and cold spots appear in the cluster and void stacks, respectively, with a characteristic radius of 4°, corresponding to spatial scales of 100 h^{-1}Mpc. The inner circle (4° radius) and equal-area outer ring mark the extent of the compensated filter used in our analysis. Given the uncertainty in void and cluster orientations, small-scale features should be interpreted cautiously.

Measurement of DE parameters
Test of cosmological models

Evolution of the K-band LF (UKIDSS-UDS)

For high-z studies, z determination is demandatory

Cirasuolo + 08, 08043471

To summarise, the master-catalogue of sources we used for this work has been selected by using both the UKIRT WFCAM K-band and Subaru SuprimeCam z'-band images in the UDS field. For the following analysis we consider ≃50,000 sources with $K \leq 23$ over an area of 0.7 square degrees, with each source having reliable photometry (detections or upper-limits) in 16 broad-bands from the far-ultraviolet to 4.5μm.

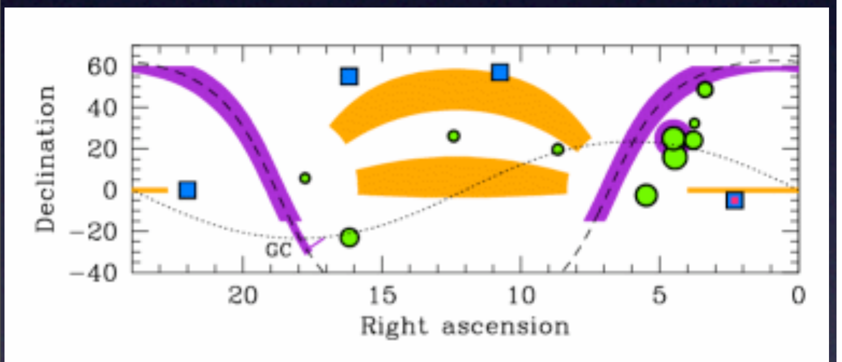

Downsizing:

bright/massive gal's are assembled at high z (1-3) and then passively evolve, while the formation of less L gal's is progressively shifted to lower z's

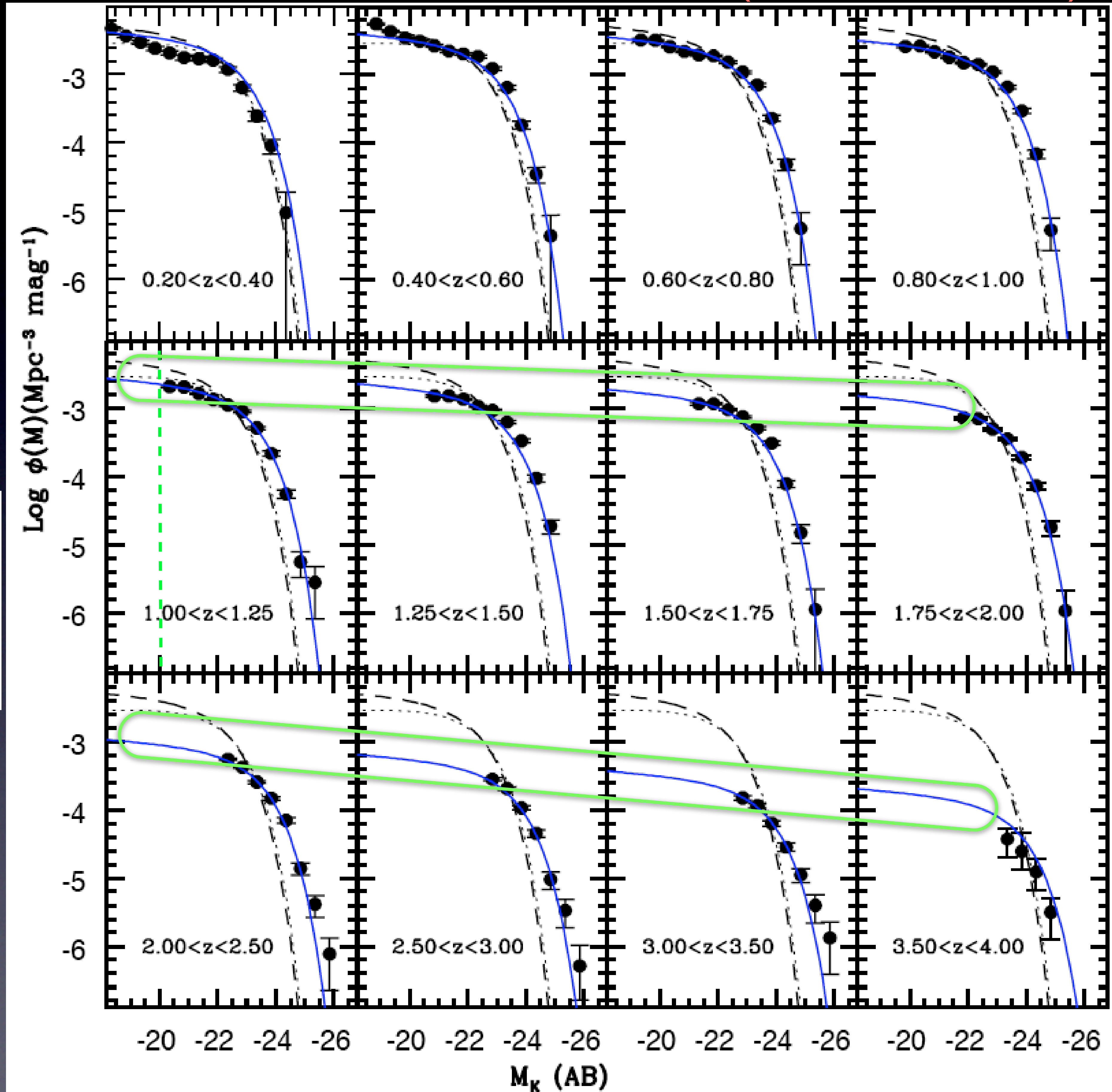

Models vs observations: a great challenge

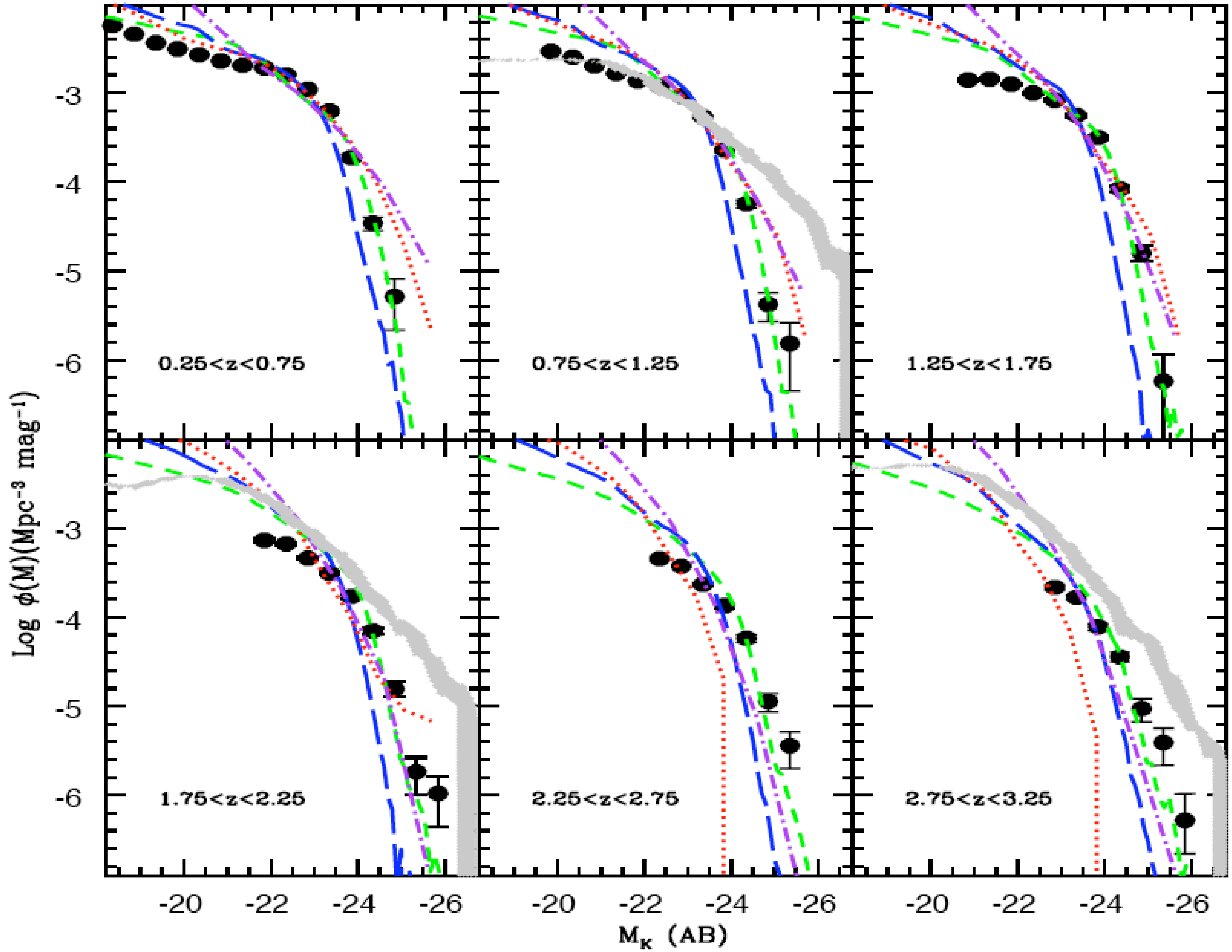

Figure 6. Comparison of our determination of the K-band LF (solid dots) with predictions of theoretical models. Short and long dashed lines are the predictions obtained by Bower et al. (2006) and De Lucia & Blaizot (2007), respectively. The predictions by Monaco et al. (2007) and Menci et al. (2006) are shown with a red dotted curve and purple dot-dashed curve, respectively. The gray area shows the prediction obtained by hydrodynamical simulations (Nagamine et al. 2006; Cen & Ostriker 2006).

Evolution of the galaxy pair fraction (merging rate)

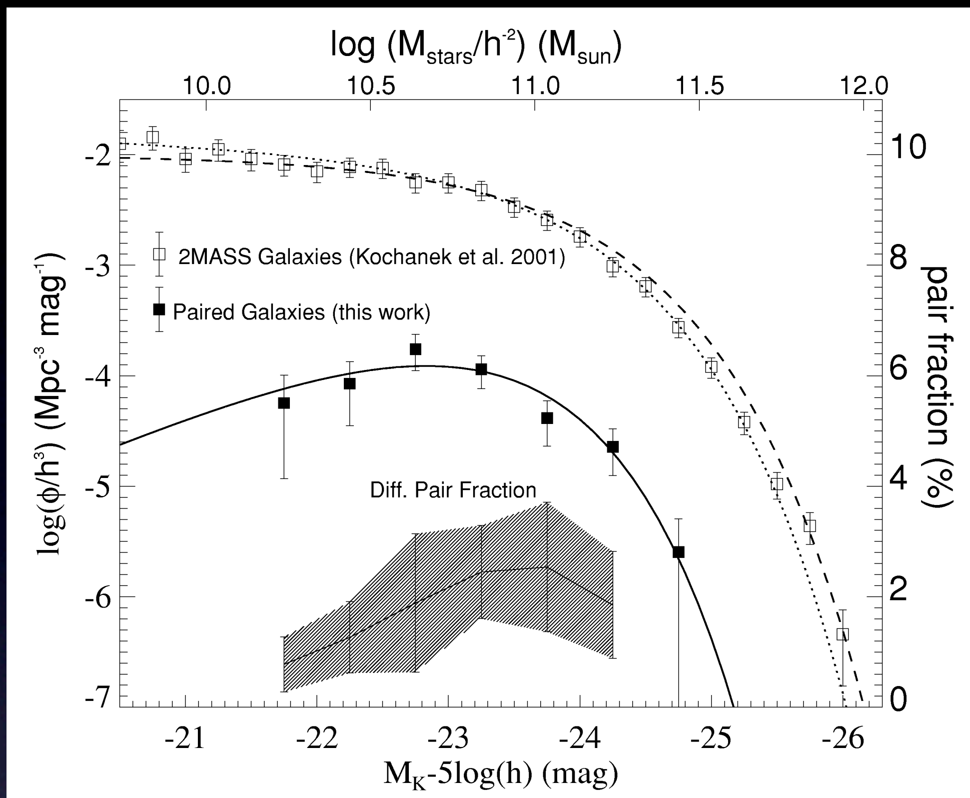

FIG. 2.—K_s-band LFs and stellar mass functions and differential pair fraction (*right coordinates*). The lines are Schechter functions of the LF of paired galaxies (*solid*), of the LF of 2MASS galaxies by Kochanek et al. (2001; *dotted*), and of the LF of 2MASS galaxies by Cole et al. (2001; *dashed*). The shaded area presents the differential pair fractions and the errors.

Local pair fraction as a function of L or M in K-band (2MASS)

Xu+04, ApJ 603

TOWARD A ROBUST ESTIMATE OF THE MERGER RATE EVOLUTION USING NEAR-IR PHOTOMETRY

A. RAWAT,[1,2] FRANCOIS HAMMER,[2] AJIT K. KEMBHAVI,[1] AND HECTOR FLORES[2]

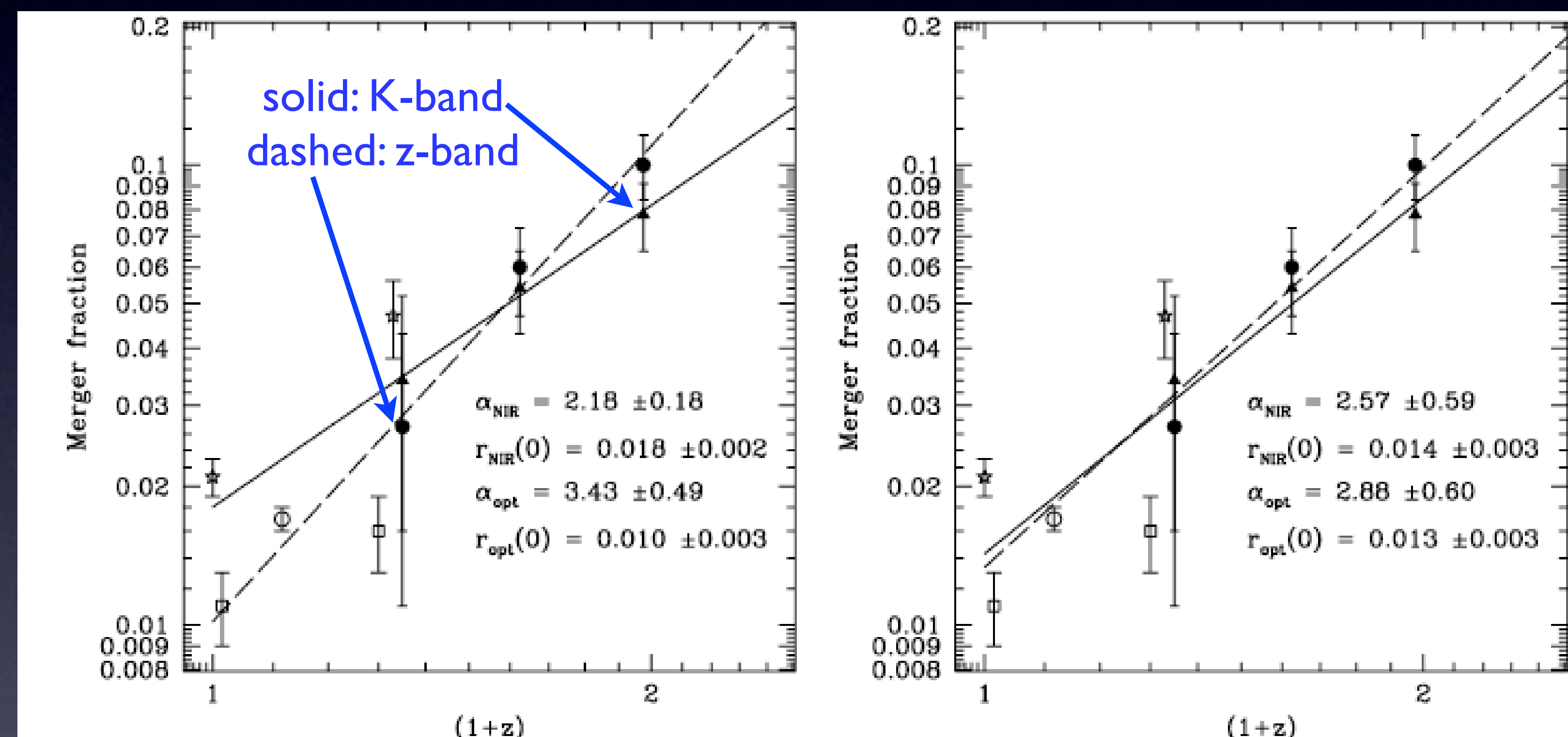

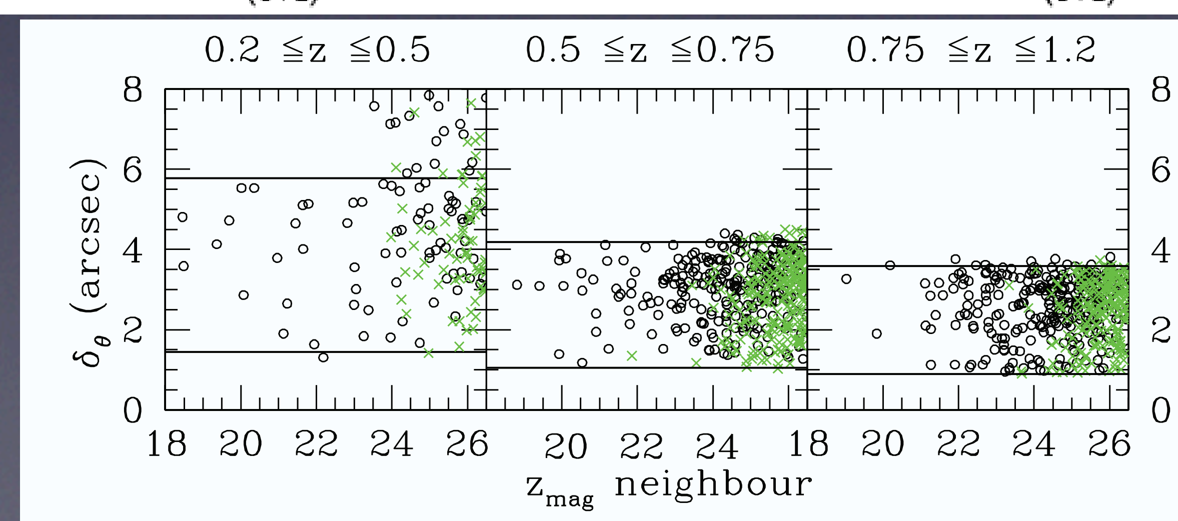

The merging rate history is an important constrain to models.

High ang. resolution needed

On the evolution of clustering of 24-µm-selected galaxies

M. Magliocchetti,[1,2,3★] M. Cirasuolo,[4] R. J. McLure,[4] J. S. Dunlop,[4]
O. Almaini,[5] S. Foucaud,[5] G. De Zotti,[3,6] C. Simpson[7] and K. Sekiguchi[8]

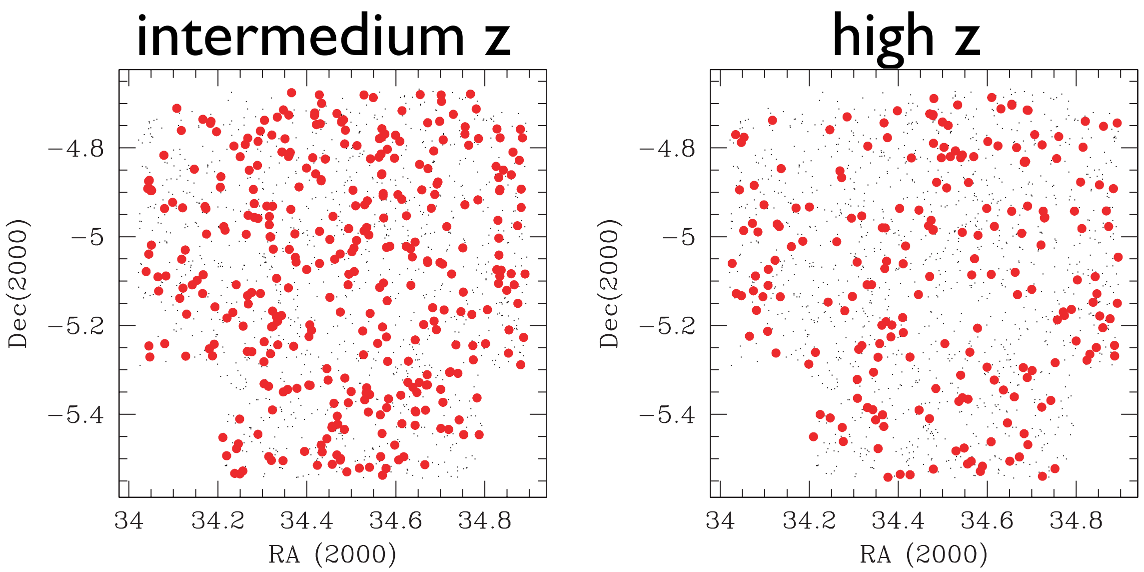

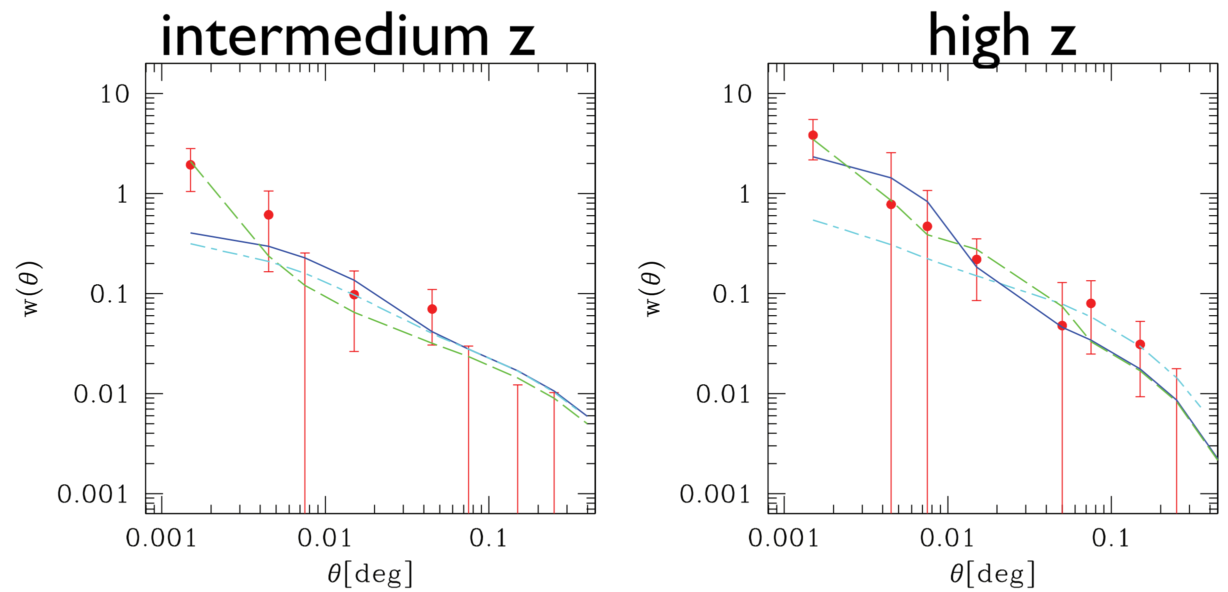

Figure 3. Sky distribution of UDS-SWIRE, $F_{24\,\mu m} \geqslant 400$ µJy sources (small dots). The filled (red) circles in the left-hand panel illustrate the 350 objects included in the redshift interval $z = [0.6–1.2]$, while those in the right-hand panel represent the 210 sources with either $z > 1.6$ or no optical or near-IR identification.

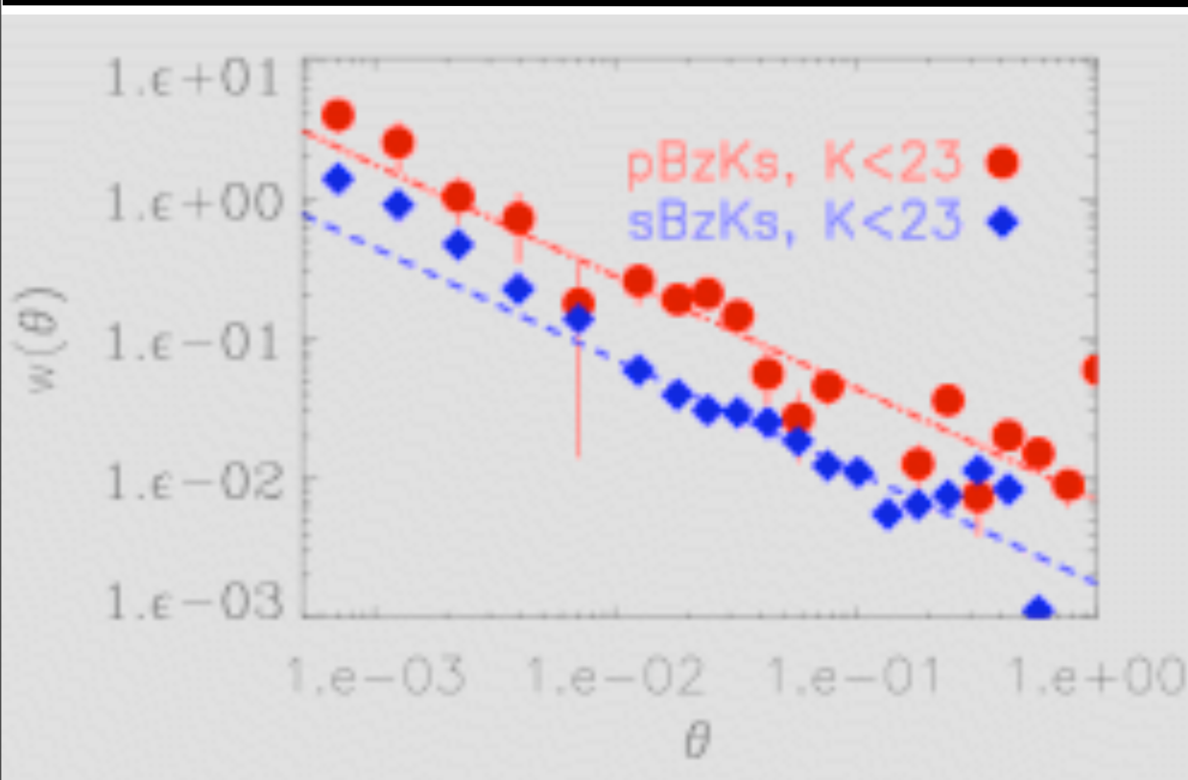

The clustering of BzK galaxies (Hartley et al., in prep.). Galaxies in the UDS have been selected to lie in the redshift range 1.4 < z < 2.5 and can be characterised as either star-forming (sBzK) or passive (pBzK) by the Daddi et al. (2004) criteria. In this redshift range it is the passive galaxies that are found to be the more highly clustered. The clustering of a set of galaxies can be directly linked to the mass of the dark matter halos in which they reside; in the case of the pBzKs the dark matter halos have mass in excess of 10^{13} solar masses.

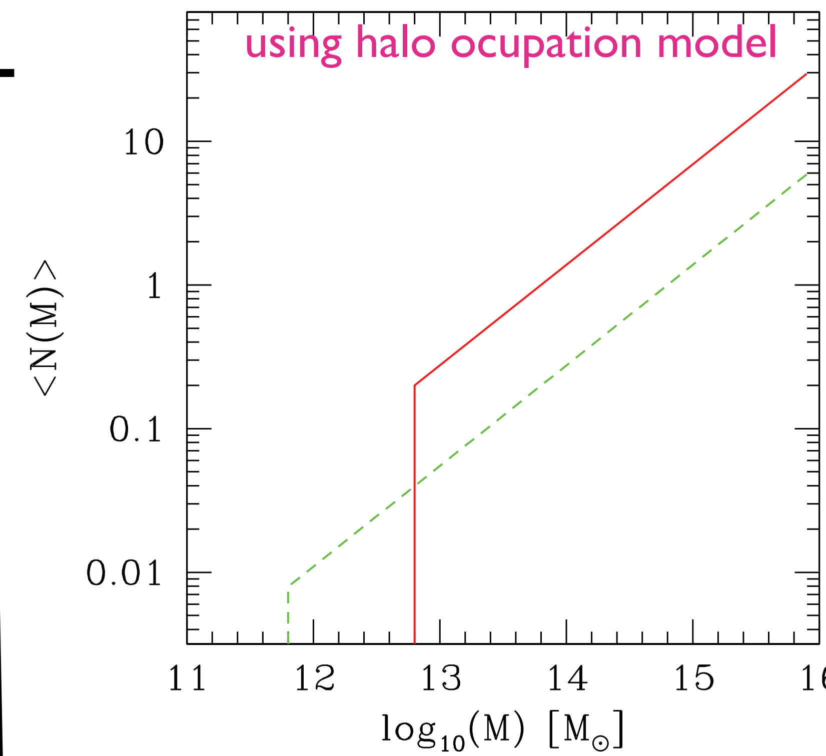

NIR color selection of high-z gal. populations

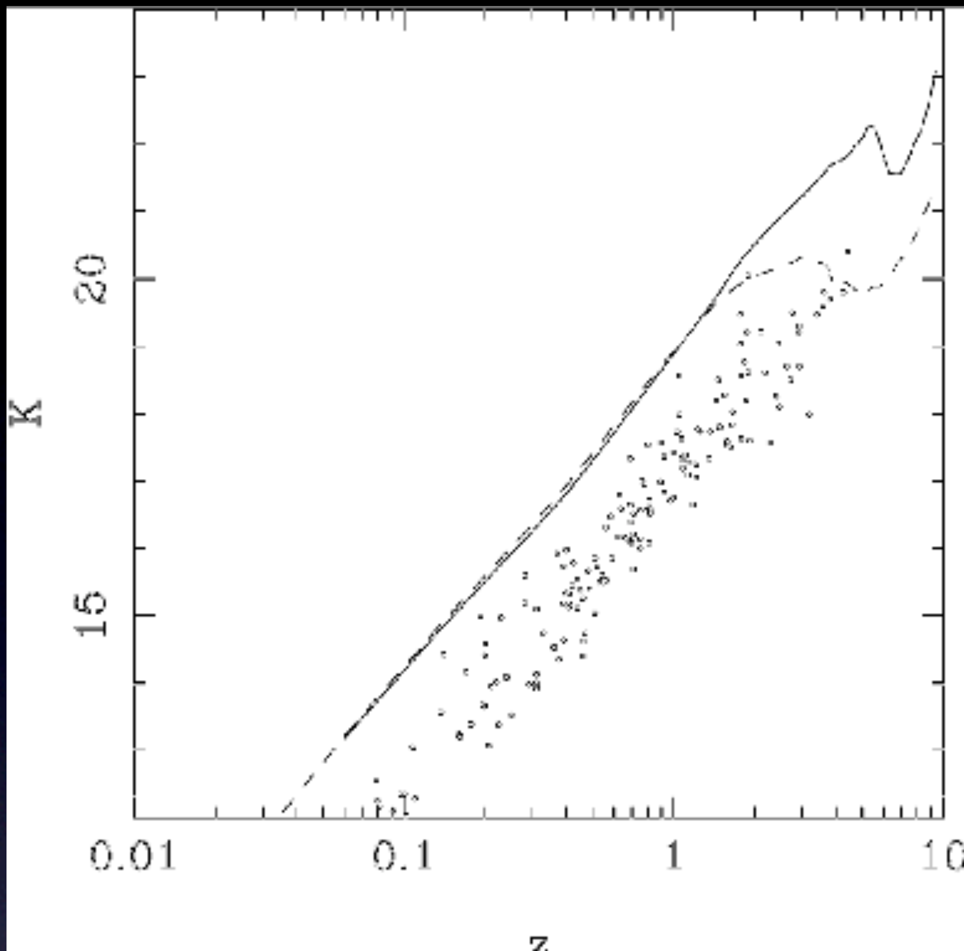

Predicted K-z Hubble diagrams for passively evolving L* ellipticals, produced by J.S. Dunlop (based on the models of Jimenez et al. 1999). Both models assume a formation redshift z_f=10. The model shown by the dashed line shows residual star formation to z=3, with a more rapid burst of star formation for the solid line (terminating at z=5). For comparison, the data points illustrate the observed K-z relation for the hosts of powerful radio galaxies (corresponding to 4×L* ellipticals).

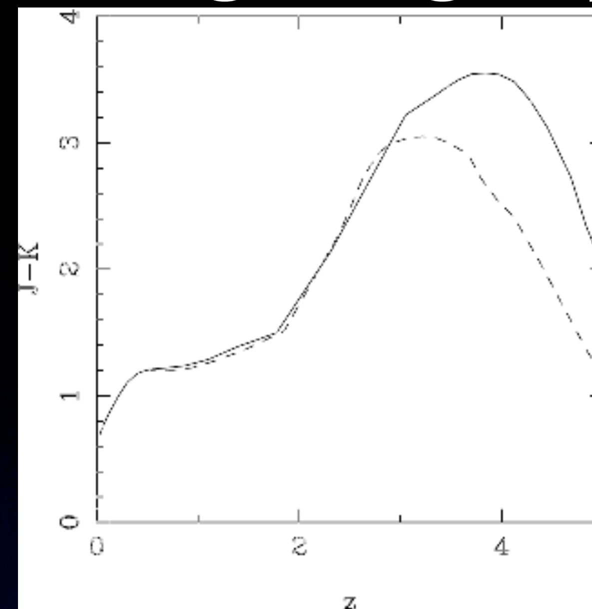

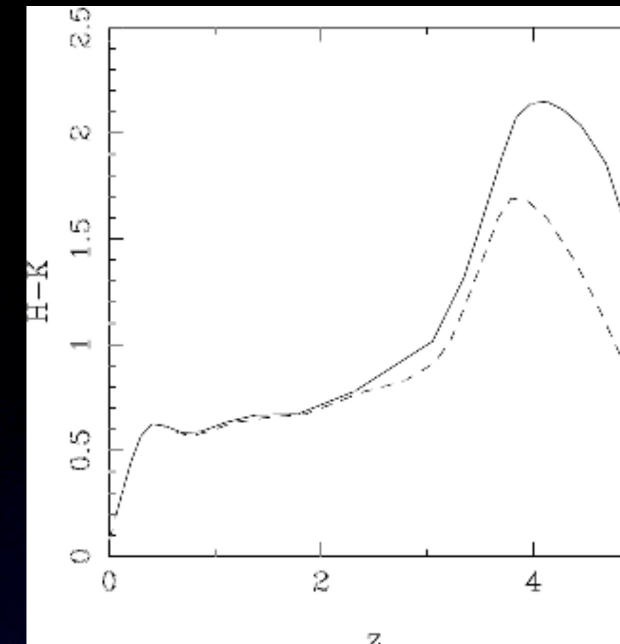

Colour information is also vital for discriminating between objects, and for the determination of photometric redshifts, particularly using the 4000Å break as it moves through the I, J, & H bands over the range 1<z<4. Photometric redshifts need two points longward of the 4000Å break and so should work up to roughly z=3. To effectively separate passive ellipticals from starbursts, we need to be able to detect colours of J-K ~3 and H-K ~1.5, otherwise the majority of our sample objects may be K-band detections only. By the same reasoning, it is also highly desirable to obtain very deep I-band data to complement the UDS. For an ERO detection, depths of I~27-28 will be required to match the above. SuprimeCam on Subaru would be ideal for such imaging.

The colour selection of distant galaxies in the UKIDSS Ultra Deep Survey Early Data Release Lane+ 08, MNRAS

Photometric redshifts for the Dark Energy Survey and VISTA and implications for large-scale structure

Manda Banerji,[1★] Filipe B. Abdalla,[1] Ofer Lahav[1] and Huan Lin[2]

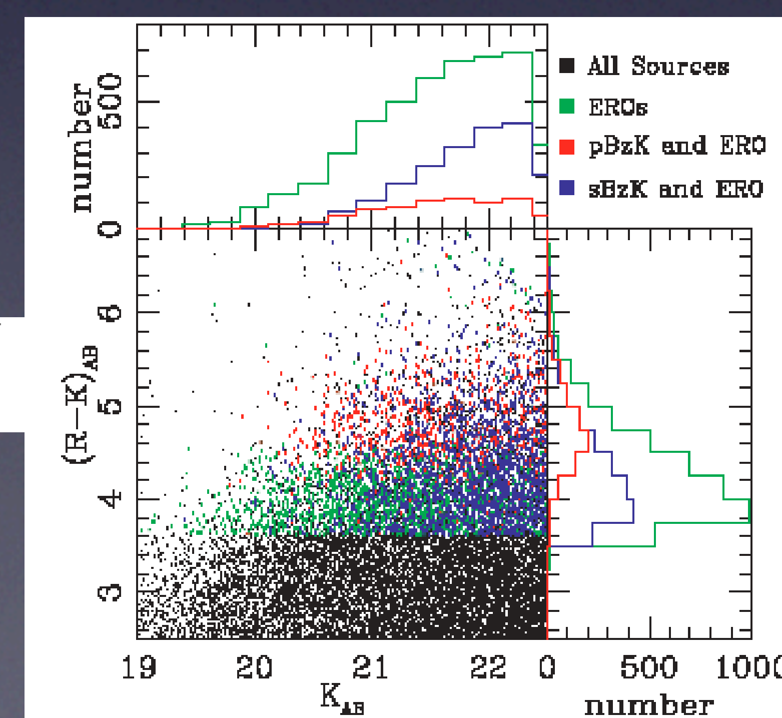

Concluding remarks

- Many EG problems could be solved with a deep and LA NIR survey
- Synergy with SMM/Opt/X-ray deep surveys will be crucial for z determination and selection of high-z objects.
- Synergy with HI surveys will allow to get baryonic quantities (the dream of modelers)
- Follow-up (spectra, opt. bands, etc.) of discovered high-z galaxies.